THE METRO VANCOUVER SEISMIC MICROZONATION MAPPING PROJECT

ISSN 2816-6027

Compilation and systematic processing of earthquake and microtremor HVSR amplification at Metro Vancouver strong-motion stations

Jamal Assaf, Aamna Sirohey, Hadi Ghofrani, Sheri Molnar

Contact us:
The Metro Vancouver Seismic Microzonation Mapping Project
University of Western Ontario
Department of Earth Sciences Biological & Geological Sciences Building (BGS 1040)
London, ON N6G 2V4
Phone: 519-661-2111 x87031

Report MVSMP-22-05

2022-05-04

Intorduction

All available earthquake recordings at strong-motion stations in Metro Vancouver are compiled and consistently processed to provide earthquake Fourier horizontal-to-vertical spectral ratios (HVSR). Earthquake recordings are obtained from Natural Resources Canada (NRCAN) including recordings from and previous to 2001 at British Columbia (BC) Hydro stations, and the BCSIMS network operated by BC Ministry of Transportation and Infrastructure (MOTI). In addition, microtremor recordings performed "at" (from co-located to within 100 m of) strong-motions stations, prior to and as part of the Metro Vancouver seismic microzonation mapping project (https://metrovanmicromap.ca), are also consistently processed to provide microtremor Fourier HVSRs. The earthquake and microtremor HVSRs provide a measure of fundamental site frequencies ($f_{\#HV}$ where $_{\#}$ is mode number; site period $T=1/f_0$) and an indication of the site (surface-to-bedrock) amplification spectrum for each strong-motion station. Selected results from this report's compilation of observed earthquake and microtremor HVSR amplification are published in Molnar et al. (2020).

The available recorded earthquakes in Metro Vancouver include time series from 12 earthquakes (Table 1). Individual earthquake events and their associated strong-motion recordings are documented in Weichert et al. (1980) and Open File reports (OF3390, OF3599, OF1737, OF5010). Analyses of the datasets are presented in Cassidy et al. (1997), Rogers et al. (1998), Cassidy and Rogers (1999), Cassidy and Rogers (2004), and Jackson et al. (2017). The 2018 earthquake had a low signal to noise ratio.

Table 1. Details of earthquakes recorded by Metro Vancouver strong-motion stations.

Latitude	Longitude	Depth (km)	Magnitude type[1]	Magnitude	Description	Year	Label
48.8	-123.4	62	**M**	5.3	Near/below Pender Island	1976	1976
47.7608	-121.876	4.4	M_L	5.5	38 km ENE of Seattle, WA. Felt	1996	1996
49.237	-123.621	3.3	**M**	4.6	20 km SW of Gibsons, BC. Felt	1997	1997
47.1548	-122.713	55.9	**M**	6.8	57 km SW of Seattle, WA. Felt	2001	2001
49.5236	-127.241	29.5	**M**	5.8	84 km W of Gold R., BC. Felt.	2004	2004
49.4746	-127.251	23.4	**M**	6.4	86 km W of Gold R., BC. Felt.	2004-2	20042
48.5654	-123.533	44.4	M_L	3.6	Near Victoria, BC. Felt	2006	2006
48.3282	-123.204	46.2	**M**	4	16 km ESE of Victoria, BC. Felt	2006-2	20062
49.3469	-127.215	35.5	**M**	6.3	88 km WSW of Gold R., BC. Felt	2011	2011
49.6388	-127.732	10	**M**	6.5	117 km W of Gold R., BC. Felt.	2014	2014
48.6151	-123.286	57.5	**M**	4.7	9 km ESE of Sidney, BC. Felt	2015	2015
49.05	-129.883	10	**M**	6.5	254 km SW of Pt. Hardy, BC	2018	2018

[1]**M** is moment magnitude, M_L is local magnitude. WA is Washington State, BC is British Columbia.

Prior to the 2001 Nisqually, WA earthquake, relatively few trigger-based strong-motion stations were operating in British Columbia. Post-2001, continuously recording Internet Accelerometers (IAs) were developed by NRCAN (Rosenberger et al. 2004) and deployed throughout southwestern BC including the CUSP grid of 7x9 stations (station codes starting with VNC and RMD) across the northern limit of the Fraser River delta in Metro Vancouver. Table 2 summarizes the strong-motion stations that recorded one or more of the 12 earthquakes listed in Table 1. Information on the site conditions at each trigger-based station can be obtained from GSC Open File reports (OF3390, OF3599, OF1737, OF5010). An assigned 'soft' site condition corresponds to post-glacial sediments with relatively low compression and shear velocities that are greater than about 20 m in thickness. The 'stiff' site condition corresponds to glacially overridden Pleistocene deposits or post-glacial sediments of less than 20 m in thickness. Original coordinates of older stations (from Open File reports) and some of the IA stations (from BCSIMS) were reviewed and updated based on the known addresses and/or field inspections. f_{0HV} range is assigned to stations with relatively reliable earthquake and microtremor HVSR.

Table 2. Details of strong-motions stations with earthquake recordings (1976-2018).

Station ID	Latitude (°N), Longitude (°E)	Earthquakes Recorded	Site conditions	f_{0HV} range (Hz)
ANN (replaced by DLT02NA in 2001)	49.1814, -122.92976	1976, 1997, 2001, 2006, 20062, 2011, 2018	Soft	0.4-0.5
ARN decommissioned in 2001	49.0912, -123.0418	1996, 1997, 2001	Soft	0.2-0.3
DEAS (replaced by RMD13 in 2001)	49.12398, -123.08178	1997, 2006, 20062, 2011, 2014, 2015	Soft	0.2-0.25
KID decommissioned in 2001	49.19852, -123.11464	1996, 1997, 2001	Soft	-
LNG01	49.102, -122.659	2006, 2011, 2014, 2015	Soft	0.8-1.0
PMB02A2	49.22551, -122.81573	2015	Soft	0.25-0.35
PMB04A4	49.21509, -122.81179	2015	Soft	0.2-0.3
PMB10C2	49.22835, -122.83404	2015	Soft	-
RHA decommissioned in 2001	49.16321, -123.13782	1996, 1976, 1997, 2001	Soft	0.2-0.25
RMD01C6	49.19657, -123.11131	2004, 20042, 2006, 20062, 2011, 2014, 2015, 2018	Soft	0.25-0.3
RMD02C7	49.183, -123.116	2004, 20042, 2006, 20062, 2011, 2015, 2018	Soft	0.2-0.3
RMD03E7	49.185, -123.09	2004, 20042, 2006, 20062, 2011, 2015, 2018	Soft	0.5-0.6
RMD04B9	49.164, -123.127	2004, 20042, 2006, 20062, 2011, 2015, 2018	Soft	0.2-0.3
RMD05C9	49.1647, -123.11871	2004, 20042, 2006, 20062, 2011, 2014, 2015, 2018	Soft	0.2-0.3
RMD06A9	49.165, -123.142	2004, 20042, 2006, 20062, 2014	Soft	0.2-0.3

RMD09A8	49.17316, -123.13972	2004, 20042, 2006, 20062, 2011, 2014, 2015	Soft	0.2-0.3
RMD11B8	49.17464, -123.12762	2006, 2014, 2015, 2018	Soft	0.2-0.3
RMD12G6	49.198, -123.059	2006, 20062, 2011, 2015, 2018	Soft	0.5-0.6
RMD14NA	49.1306, -123.18236	20062, 2011	Soft	0.2-0.25
RMD15NA	49.171, -123.185	20062, 2011, 2014, 2015, 2018	Soft	0.2-0.25
RMD16NA	49.14849, -123.14898	20062, 2011, 2015	Soft	0.2-0.25
ROB decommissioned in 2001 (Replaced DLT01NA)	49.02072, -123.15561	1976, 2006, 20062, 2011	Soft	0.3-0.4
SNB01NA	49.301, -123.026	2014, 2015, 2018	Soft	0.6-0.7
VNC09A6	49.191, -123.15	2004, 20042, 2006, 20062 , 2014, 2015	Soft	0.2-0.3
BND decommissioned in 2001	49.26255, -122.9001	1996, 1997, 2001	Stiff	1.8-1.9
CLE decommissioned in 2001	49.36016, -123.11048	1997	Stiff	4.5-5.0
CSQ decommissioned in 2001	49.2826, -123.11351	1997, 2001	Stiff	
EBT decommissioned in 2001	49.0076, -123.08877	1996, 2001	Stiff	0.3-0.4
ING decommissioned in 2001	49.1586, -122.8739	2001	Stiff	
MDN decommissioned in 2001	49.3089, -122.8058	1996, 1997, 2001	Stiff	2.5-3.5
MNY decommissioned in 2001	49.2084, -123.11135	1996, 1997, 2001	Stiff	0.5-0.6
MUR decommissioned in 2001	49.27815, -123.10134	1997	Stiff	4.0-5.5
SFU01NA	49.279, -122.915	2006, 2011, 2018	Stiff	
UBC decommissioned in 2001 (replaced by UBC01)	49.263, -123.25	2001, 2006, 20062, 2011, 2014, 2015, 2018	Stiff	0.8-0.9
VNC01G2	49.23, -123.054	2004, 20042, 2006, 20062, 2011, 2014, 2015	Stiff	0.6-0.7
VNC02D4	49.21476, -123.09663	2004, 20042, 2006, 2011, 2018	Stiff	
VNC03D1	49.24152, -123.10055	2004, 20042, 2006, 20062, 2011, 2014, 2018	Stiff	

VNC04G1	49.23713, -123.05835	2004, 20042, 2006, 20062, 2011, 2014, 2015, 2018	Stiff	
VNC05G4	49.21346, -123.05821	2004, 20042, 2006, 20062, 2011, 2014	Stiff	0.5-0.6
VNC06E4	49.21583, -123.08475	2004, 20042, 2006, 20062, 2011, 2014, 2015	Stiff	
VNC07F4	49.21489, -123.07317	2004, 20042, 2006, 20062, 2018	Stiff	
VNC10A3	49.22119, -123.14068	2006, 20062, 2014	Stiff	
VNC11G5	49.20587, -123.05666	2006, 2014	Stiff	
VNC12G3	49.22102, -123.05529	2006, 20062, 2011, 2014	Stiff	
VNC13NA	49.28712, -123.11779	2006, 20062, 2011, 2014, 2015, 2018	Stiff	
VNC14A4	49.21, -123.136	2006, 2011, 2014, 2015, 2018	Stiff	
VNC15B3	49.22068, -123.1256	2006, 20062, 2011, 2014	Stiff	
VNC16B1	49.24, -123.125	2006, 20062	Stiff	
VNC18D3	49.22263, -123.09544	2006, 20062, 2011, 2014, 2015, 2018	Stiff	
VNC19NA	49.221, -123.087	2006, 20062, 2011	Stiff	
VNC22F2	49.232, -123.068	2006, 20062, 2011, 2014, 2015, 2018	Stiff	
VNC23F1	49.23712, -123.07375	2006, 20062, 2011, 2018	Stiff	
VNC24NA	49.221, -123.071	2006, 20062, 2011, 2014, 2015, 2018	Stiff	
VNC26NA	49.276, -123.112	2011, 2014, 2015, 2018	Stiff	
BLO decommissioned in 2001	49.24195, -123.11365	1997, 2001	Volcanic rock	
HNB decommissioned in 2010	49.2745, -122.5792	2001	Granitic rock	
HNBB decommission in 2019	49.2873, -122.5729	2015	Granitic rock	
PGC decommissioned in 2001 (replaced by PGC01)	48.651, -123.451	2001, 2006, 2011, 2014, 2015	Granitic rock	

Note: HNB & HNBB are Canadian National Seismograph Network (CNSN) seismograph stations.

Calculation of earthquake HVSRs

The original time series file formats vary between ASCII, SAC, and MiniSEED. All the original time series are converted to MiniSEED format using ObsPy Python library (Beyreuther et al. 2010).

Trigger-based pre-2001 waveform files were provided by S. Molnar. The recorded time series consist of the earthquake waveform with shear and surface wave arrivals. No pre-trigger seismic noise recording exists. Often the P-wave arrivals are missing (did not trigger yet) and the time-series duration varies between ~10 to ~ 60 seconds amongst recordings (based on instrument settings). The horizontal component waveforms were rotated according to the earthquake epicentre's azimuth from the station (termed radial or SV and tangential or SH components). No further processing or filtering is applied to these earthquake waveforms.

For IA stations, the 2004 and 2004-2 earthquake time-series were processed by Molnar et al. (2004). The recorded time series are downloaded at a default two-minute duration and thereby include the earthquake waveform. The provided north and east horizontal components are rotated to radial and tangential components. No further processing is applied to these time series. The IA recordings from 2006 to 2018 were provided as continuous time series of at least 10 minutes duration. The recordings are calibrated based on the instrument calibration factor provided by BC MOTI (e.g., Jackson et al. 2017) and then baseline corrected by removing the mean value, and detrended (linear and 2nd order). The two horizontal components are rotated to radial and tangential components based on the earthquake back azimuth of each station. A three minute time window spanning the timing of the earthquake and with the highest amplitudes (shear and dominantly surface waves) is saved; for the 2015 earthquake, a 40-sec time-series duration is used. In addition, pre-event noise time windows are selected for each earthquake recording. The two orthogonal horizontal components are rotated to radial and tangential components. For all cut waveform and noise windows, tapering with a 2% Tuckey (cosine) window is applied prior to applying an acausal 4th order Butterworth filter with a pass band of 0.05 – 40 Hz; a 5% taper window is applied to the 2015 recordings.

Fourier spectra are calculated via the fast Fourier transform, smoothed using the Konno and Ohmachi (1998) filter with a b-value of 20, and the geometric mean of the two horizontal component spectra is calculated. The waveform and noise Fourier spectra are corrected by dividing by the square root of its respective time window duration according to Perron et al. (2018). The signal-to-noise ratio (SNR) is calculated as the ratio of the corrected Fourier event spectrum with the corrected Fourier noise spectrum. The earthquake HVSR is considered valid here when the SNR is ≥ 2. At many stiff sites (e.g., VNC sites), the SNR acceptance criteria resulted in a very limited reliable HVSR frequency band near the fundamental (or higher mode) frequencies of the site. For trigger-based stations, the HVSR is not plotted at frequencies below 0.5 Hz as little energy exists at these low frequencies in the records (Cassidy and Rogers 1999).

Calculation of microtremor HVSRs

Microtremor recordings in Metro Vancouver are compiled from various sources. Microtremor recordings performed with a Guralp 40T broad-band seismometer by S. Molnar in 2004 at southern CUSP grid stations and around 2005 at BC Hydro stations (ARN, DEAS, DLT, EBT) are co-located with the strong-motion station; co-located means the microtremor recording is performed outdoors on the same property (within 10's of meters) as the strong-motion station which is located indoors. Microtremor recordings performed primarily with Tromino® seismometers by field personnel in 2018, 2019, and 2020 of the Metro Vancouver seismic microzonation mapping project are performed in a ~ 600x600 m regional grid, at ~100 seismic array sites, or co-located with a selection of IA stations. Co-located and "nearby" microtremor recordings are utilized to compare with the earthquake HVSRs for each strong-motion station; nearby means located closely (within 100 m). Microtremor recordings are of ≥ 30 minutes duration on the lowland Fraser River delta and Nicomekl-Serpentine valley and a minimum of 15 minutes duration elsewhere. Seismic passive-arrays performed within 220 m from 8 selected strong motion station (Assaf et al. 2022) are also used to calculate the average microtremor HVSR for comparison with earthquake HVSR.

All microtremor recordings are processed using Geopsy software (https://geopsy.org) with time windowing between 25 and 60 seconds. The Fourier spectra are smoothed using the Konno and Ohmachi (1998) filter with a b-value of 40 and the squared-average of the two horizontal components is calculated. For passive-arrays, the average of all individual HVSR in all spacings was calculated.

HVSR amplification at Metro Vancouver strong-motion stations

The HVSR amplification spectra from earthquake recordings at Metro Vancouver strong-motion stations are shown in the following figures. The co-located or nearby microtremor HVSR amplification spectrum is also plotted for comparison at applicable strong-motion stations. Presentation of each station's HVSR amplification is alphabetical within each site conditions category (soft, stiff, and rock sites; Table 2). In each Figure, the left panel shows the average HVSR amplification from earthquake recordings (colour lines) compared with microtremor HVSRs. The microtremor HVSR from a broadband seismometer recording (MHVSR BR) are shown in black, from a Tromino seismometer recordings are shown in grey, and the spatially averaged MHVSR from array testing are shown in dashed grey. In the right panel, earthquake HVSRs of the individual horizontal component spectra are shown.

Soft Sites

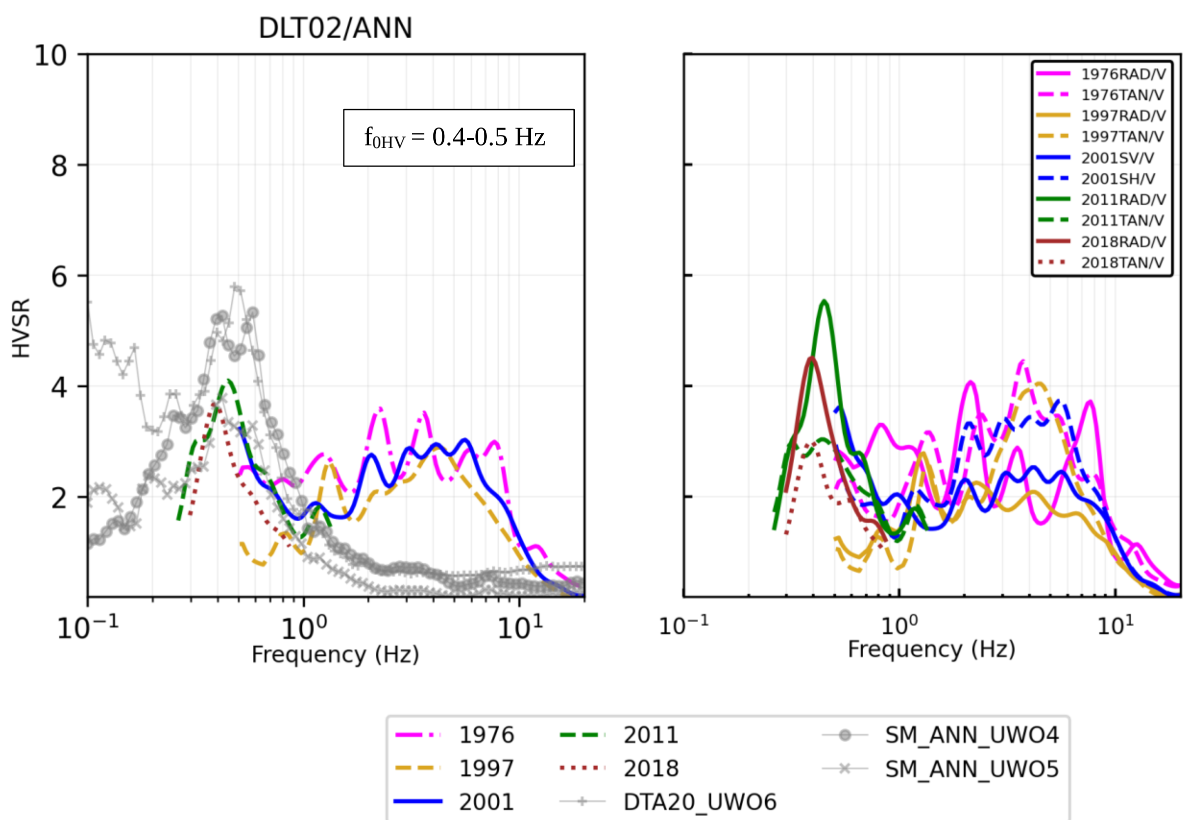

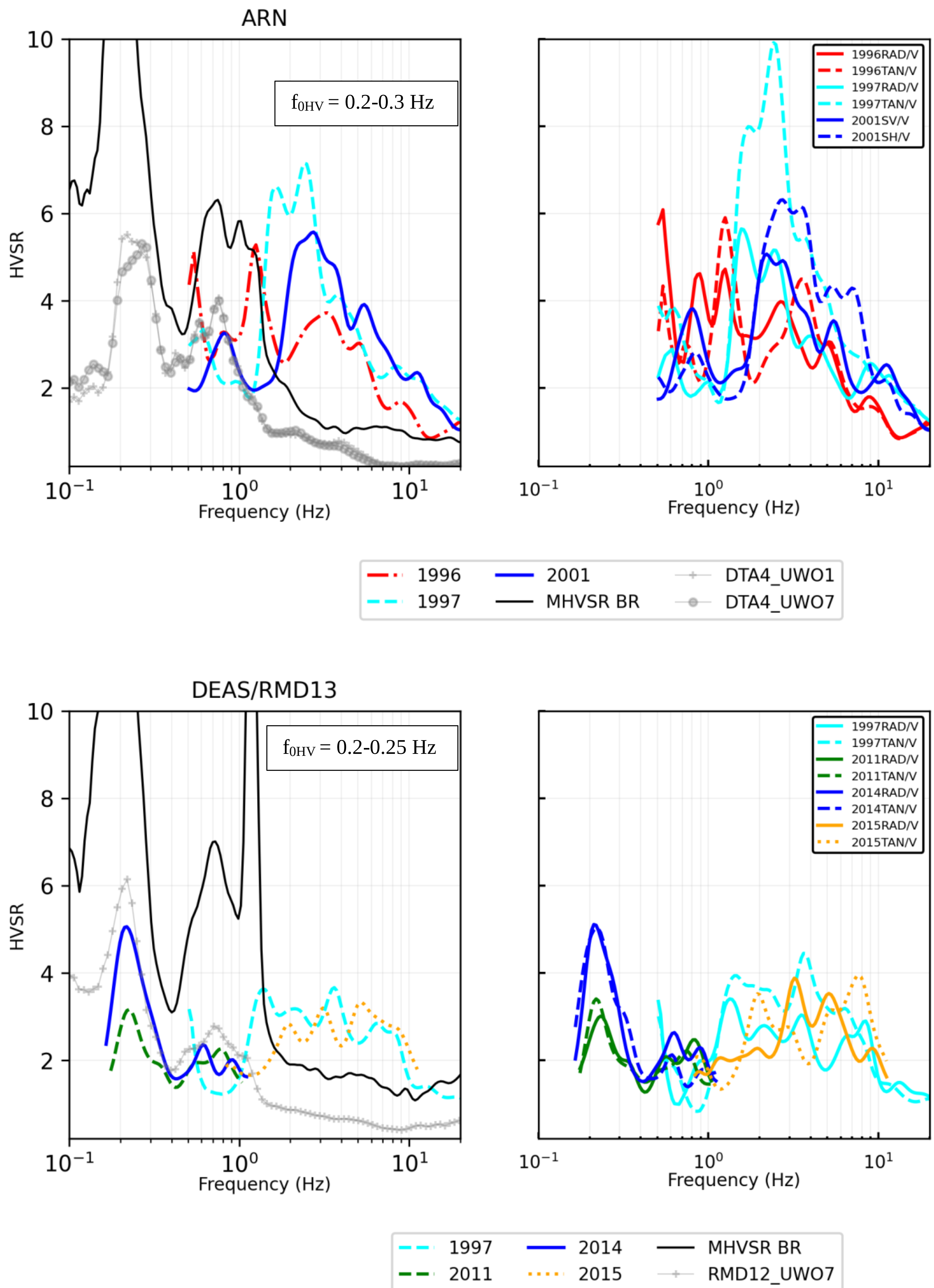
ARN
f0HV = 0.2-0.3 Hz
HVSR
Frequency (Hz)
1996RAD/V
1996TAN/V
1997RAD/V
1997TAN/V
2001SV/V
2001SH/V
1996
1997
2001
MHVSR BR
DTA4_UWO1
DTA4_UWO7
DEAS/RMD13
f0HV = 0.2-0.25 Hz
1997RAD/V
1997TAN/V
2011RAD/V
2011TAN/V
2014RAD/V
2014TAN/V
2015RAD/V
2015TAN/V
1997
2011
2014
2015
MHVSR BR
RMD12_UWO7

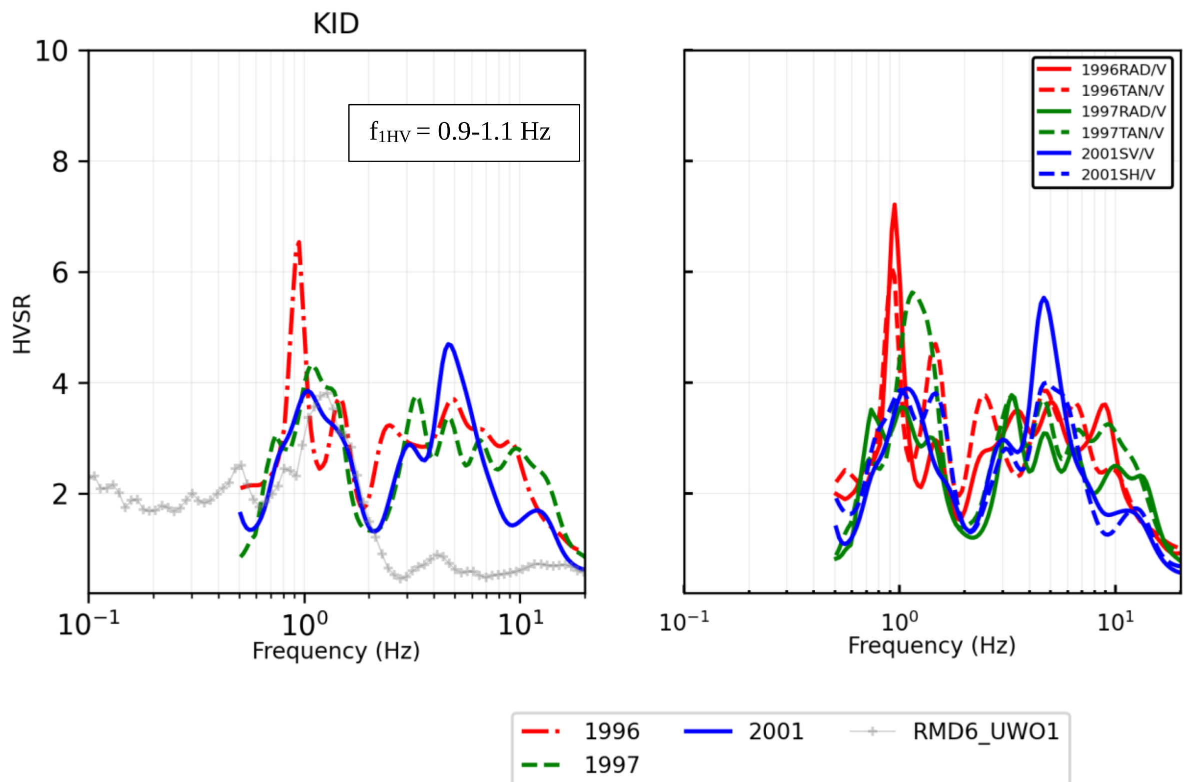
KID
f1HV = 0.9-1.1 Hz
HVSR
Frequency (Hz)
1996RAD/V
1996TAN/V
1997RAD/V
1997TAN/V
2001SV/V
2001SH/V
1996
1997
2001
RMD6_UWO1

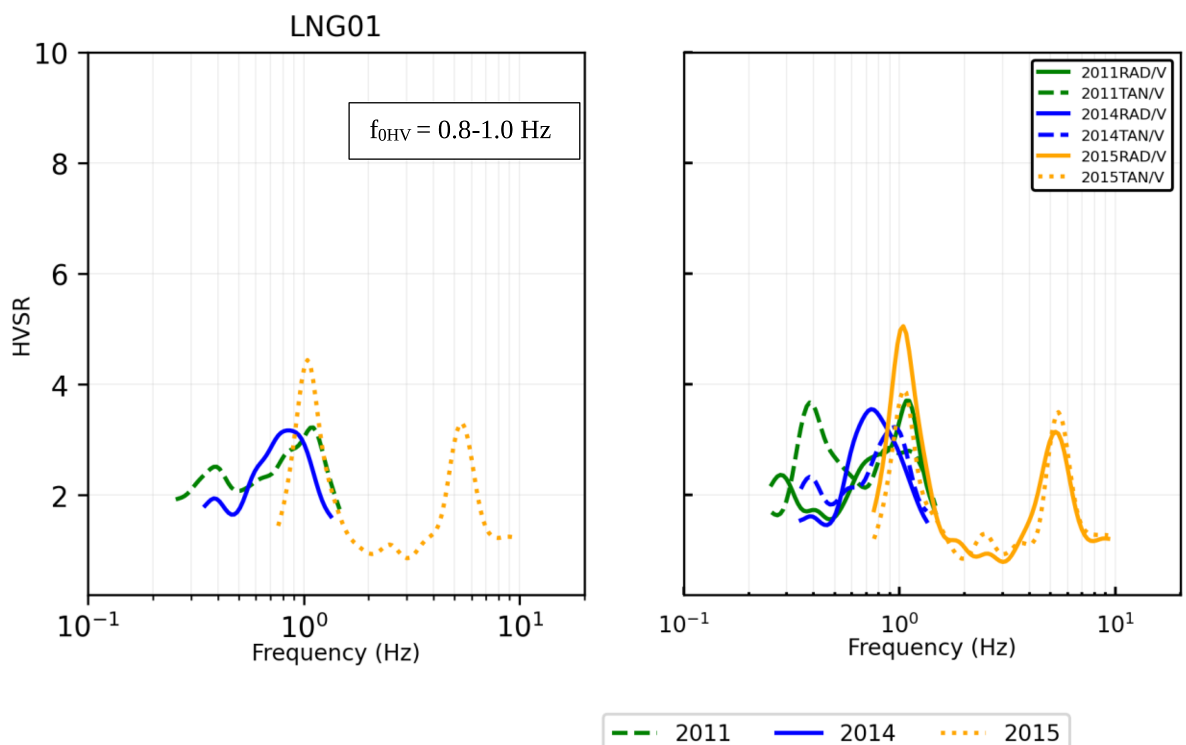
LNG01
f0HV = 0.8-1.0 Hz
HVSR
Frequency (Hz)
2011RAD/V
2011TAN/V
2014RAD/V
2014TAN/V
2015RAD/V
2015TAN/V
2011
2014
2015

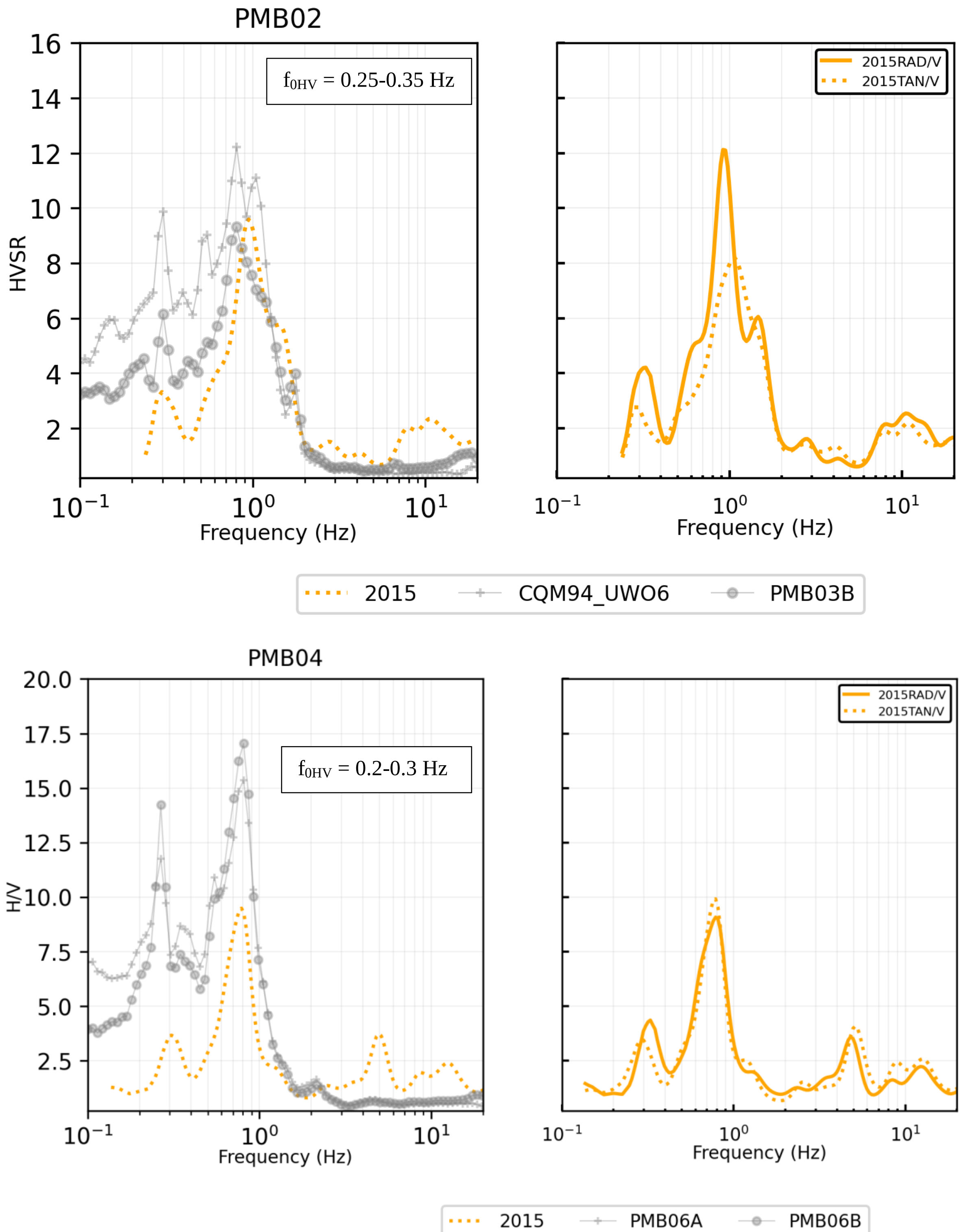
PMB02
f0HV = 0.25-0.35 Hz
HVSR
Frequency (Hz)
2015RAD/V
2015TAN/V
2015
CQM94_UWO6
PMB03B
PMB04
f0HV = 0.2-0.3 Hz
H/V
PMB06A
PMB06B

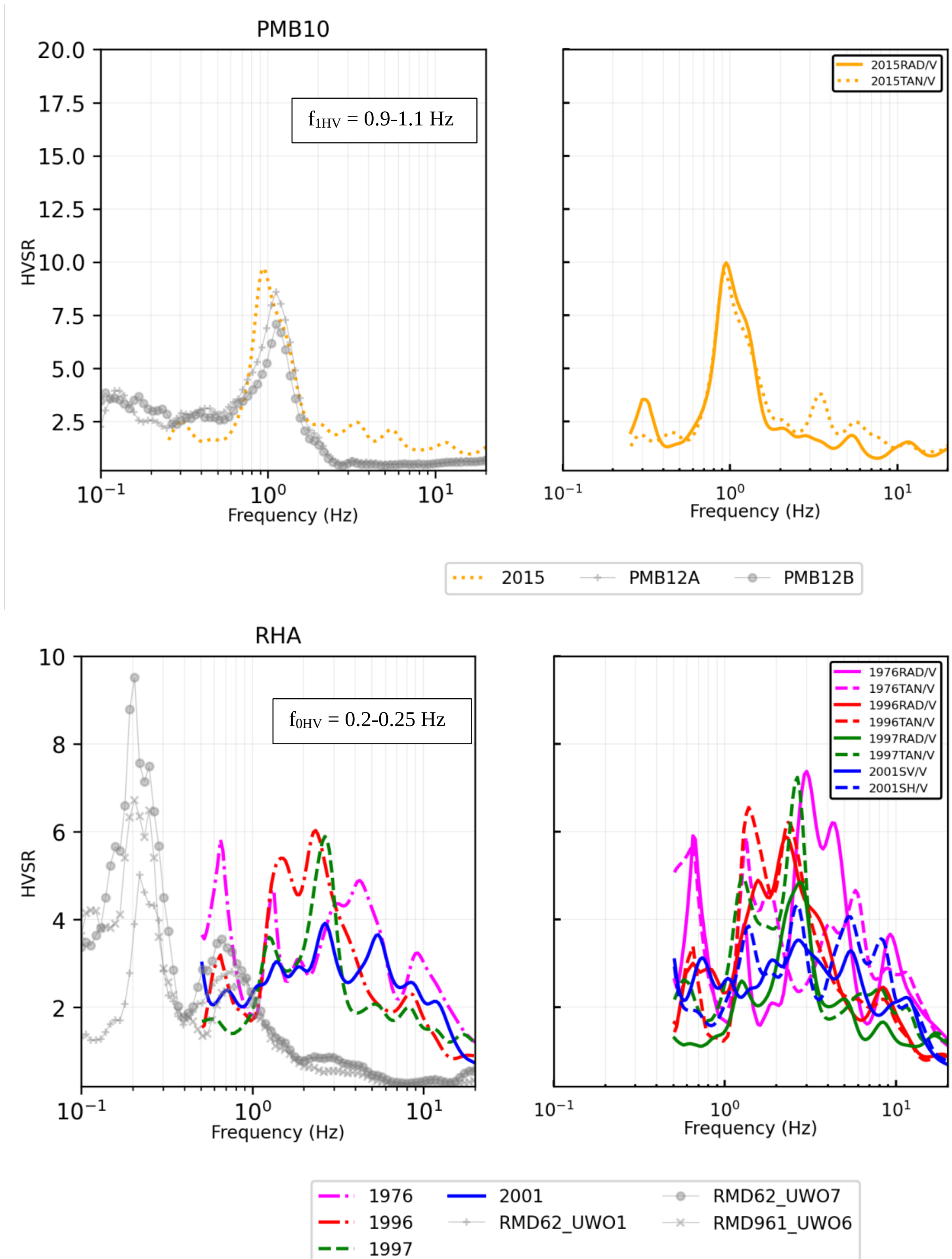
PMB10
f_{1HV} = 0.9-1.1 Hz
HVSR
Frequency (Hz)
2015RAD/V
2015TAN/V
2015
PMB12A
PMB12B
RHA
f_{0HV} = 0.2-0.25 Hz
1976RAD/V
1976TAN/V
1996RAD/V
1996TAN/V
1997RAD/V
1997TAN/V
2001SV/V
2001SH/V
1976
1996
1997
2001
RMD62_UWO1
RMD62_UWO7
RMD961_UWO6

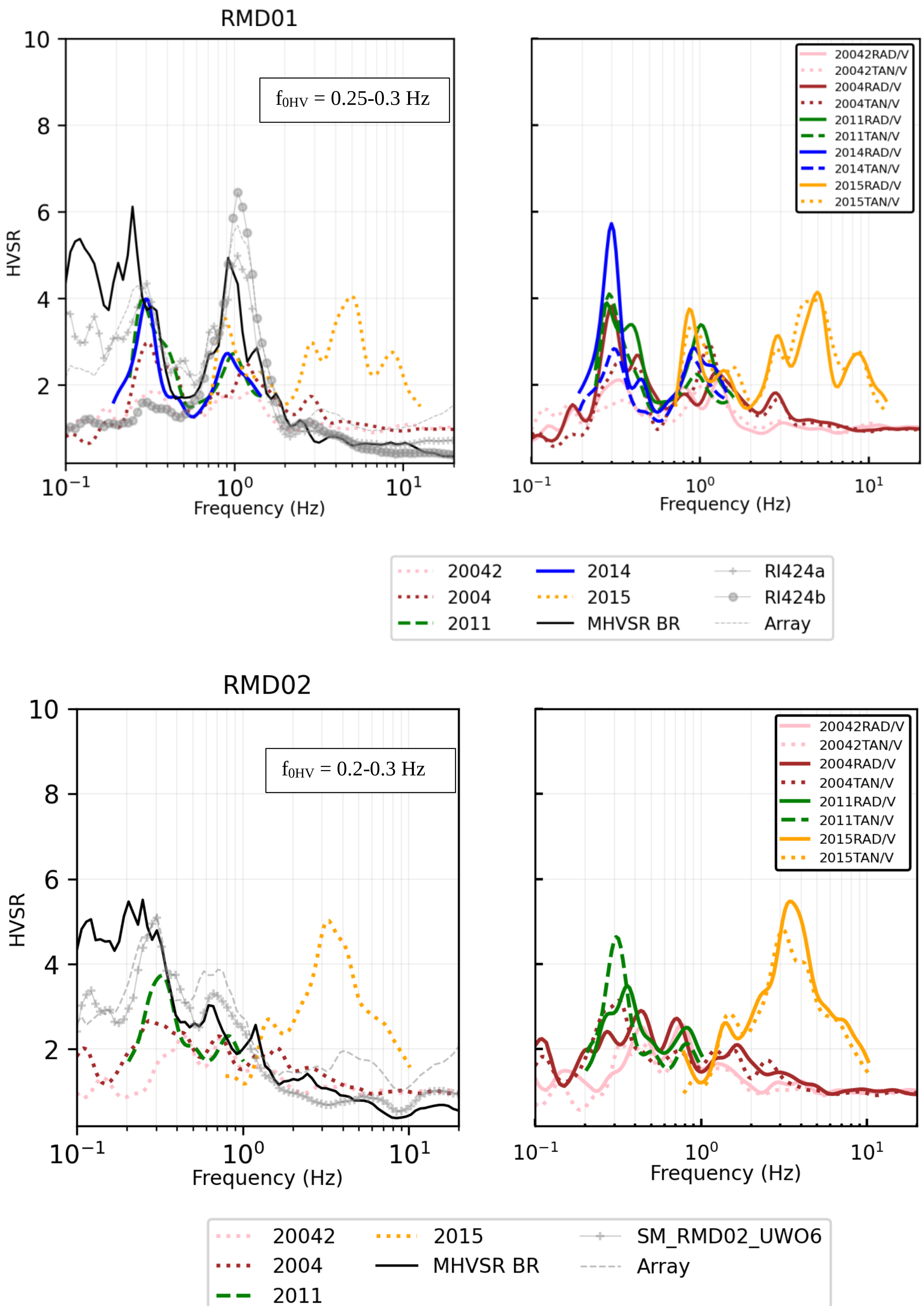

RMD01
f_{0HV} = 0.25-0.3 Hz
HVSR
Frequency (Hz)
20042RAD/V
20042TAN/V
2004RAD/V
2004TAN/V
2011RAD/V
2011TAN/V
2014RAD/V
2014TAN/V
2015RAD/V
2015TAN/V
20042
2004
2011
2014
2015
MHVSR BR
RI424a
RI424b
Array
RMD02
f_{0HV} = 0.2-0.3 Hz
HVSR
Frequency (Hz)
20042RAD/V
20042TAN/V
2004RAD/V
2004TAN/V
2011RAD/V
2011TAN/V
2015RAD/V
2015TAN/V
20042
2004
2011
2015
MHVSR BR
SM_RMD02_UWO6
Array

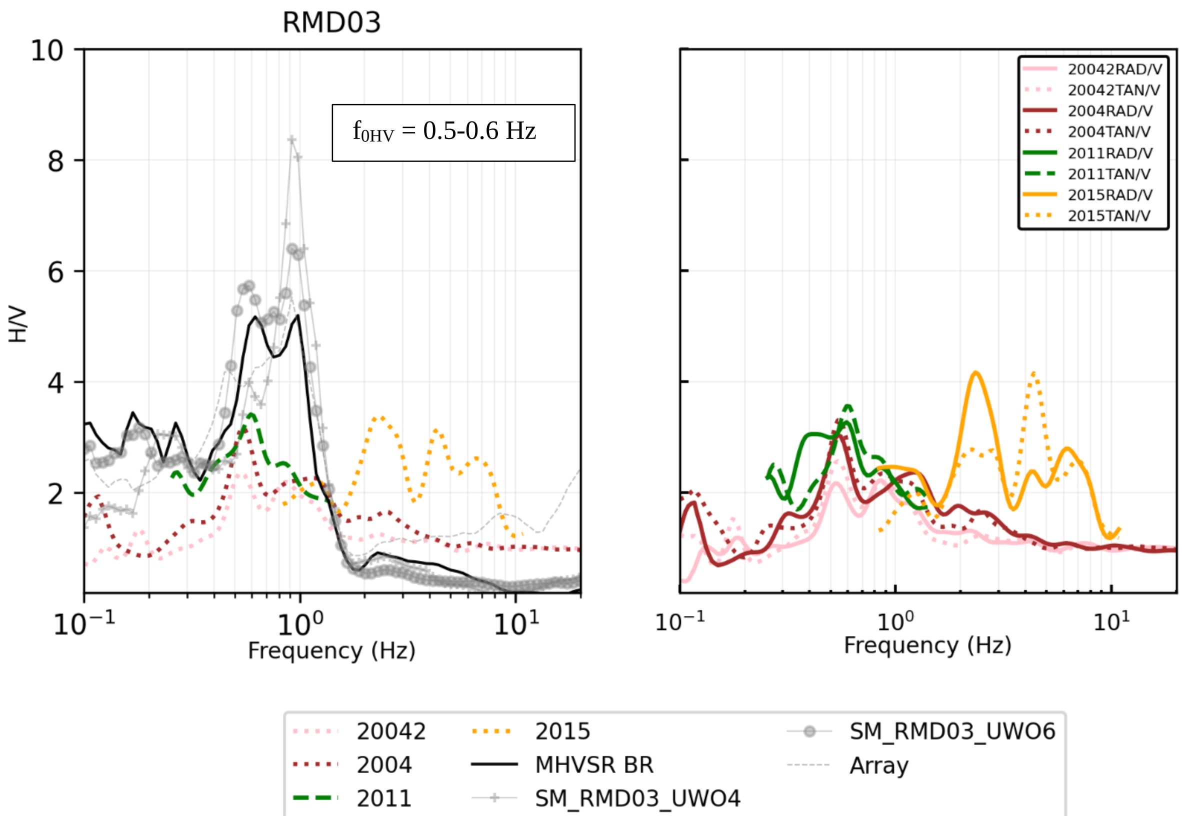
RMD03
H/V
f_{0HV} = 0.5-0.6 Hz
Frequency (Hz)
20042RAD/V
20042TAN/V
2004RAD/V
2004TAN/V
2011RAD/V
2011TAN/V
2015RAD/V
2015TAN/V
20042
2004
2011
2015
MHVSR BR
SM_RMD03_UWO4
SM_RMD03_UWO6
Array

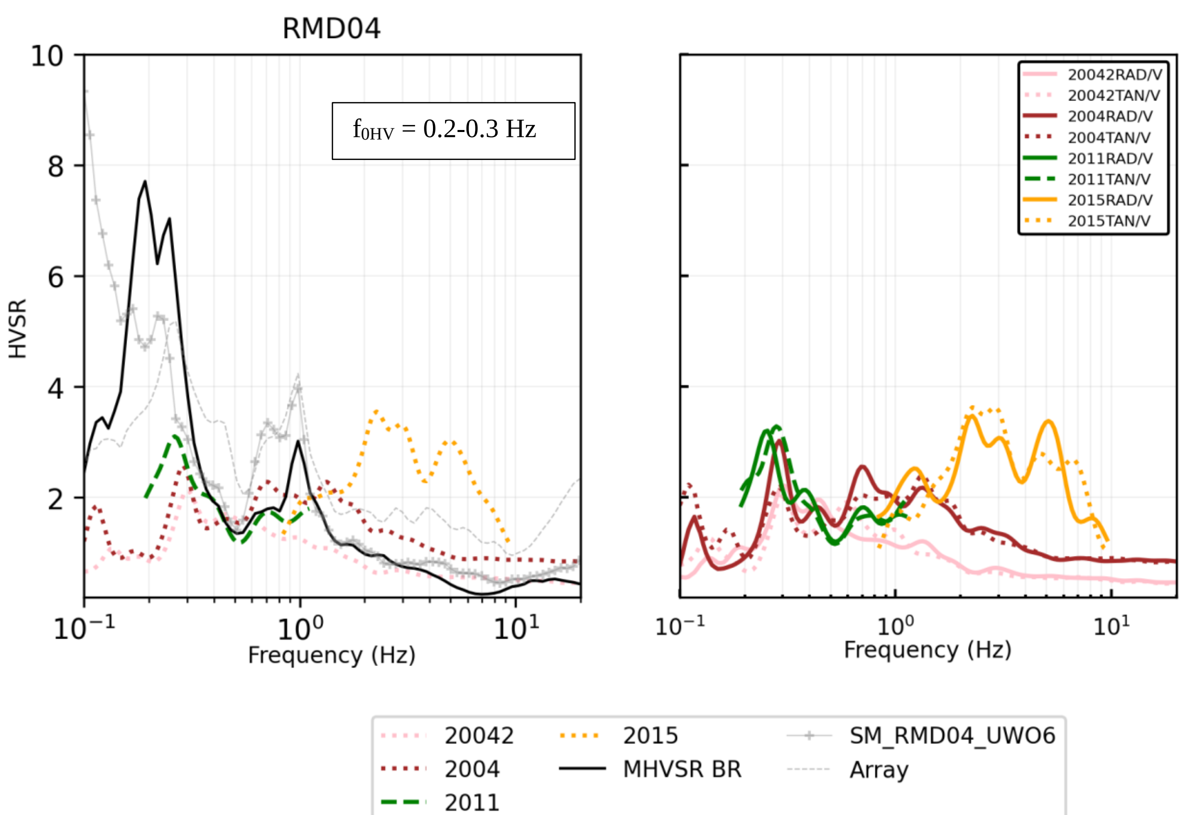
RMD04
HVSR
f_{0HV} = 0.2-0.3 Hz
Frequency (Hz)
20042RAD/V
20042TAN/V
2004RAD/V
2004TAN/V
2011RAD/V
2011TAN/V
2015RAD/V
2015TAN/V
20042
2004
2011
2015
MHVSR BR
SM_RMD04_UWO6
Array

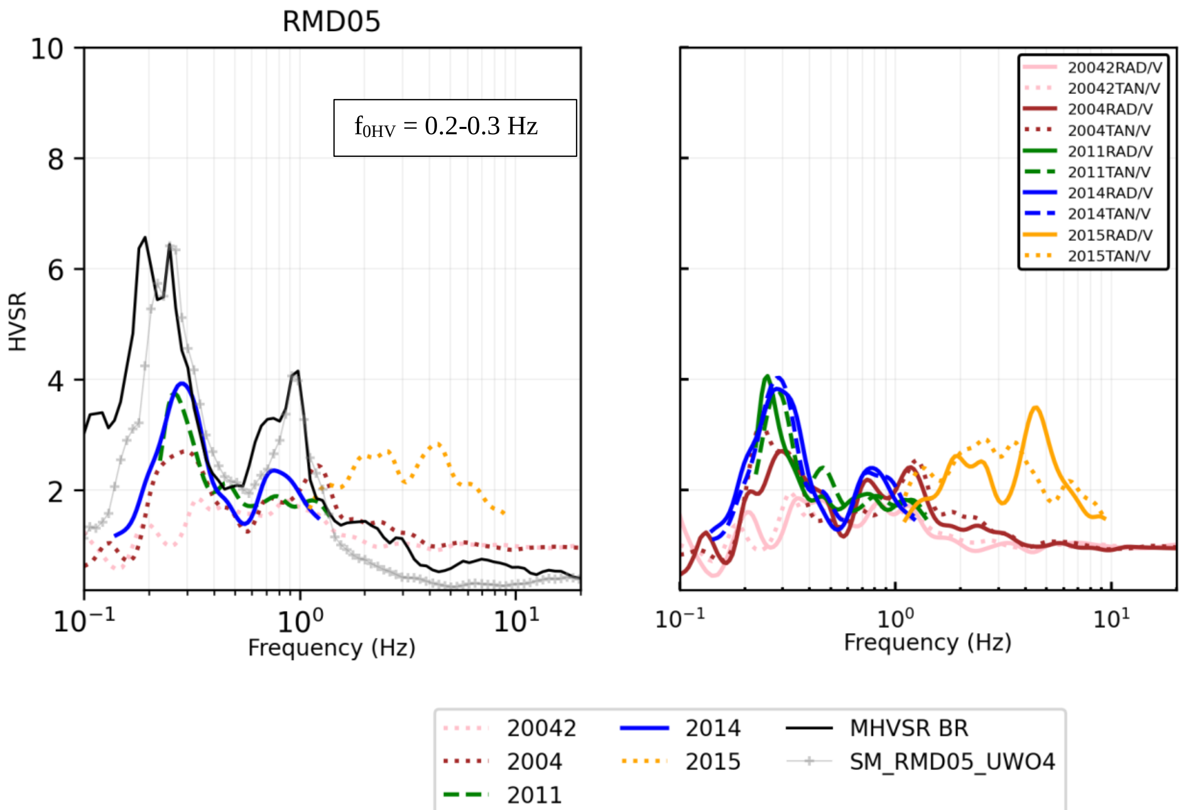
RMD05
f0HV = 0.2-0.3 Hz
HVSR
Frequency (Hz)
20042RAD/V
20042TAN/V
2004RAD/V
2004TAN/V
2011RAD/V
2011TAN/V
2014RAD/V
2014TAN/V
2015RAD/V
2015TAN/V
20042
2004
2011
2014
2015
MHVSR BR
SM_RMD05_UWO4

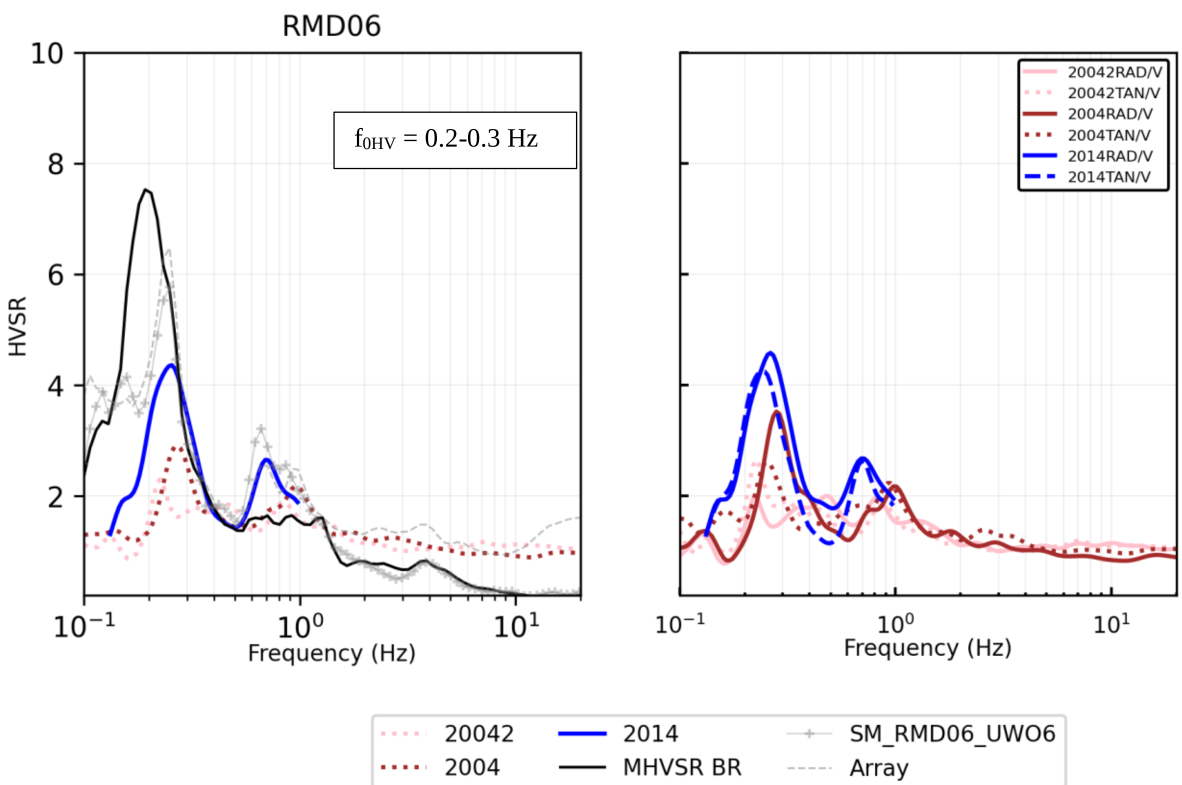
RMD06
f0HV = 0.2-0.3 Hz
HVSR
Frequency (Hz)
20042RAD/V
20042TAN/V
2004RAD/V
2004TAN/V
2014RAD/V
2014TAN/V
20042
2004
2014
MHVSR BR
SM_RMD06_UWO6
Array

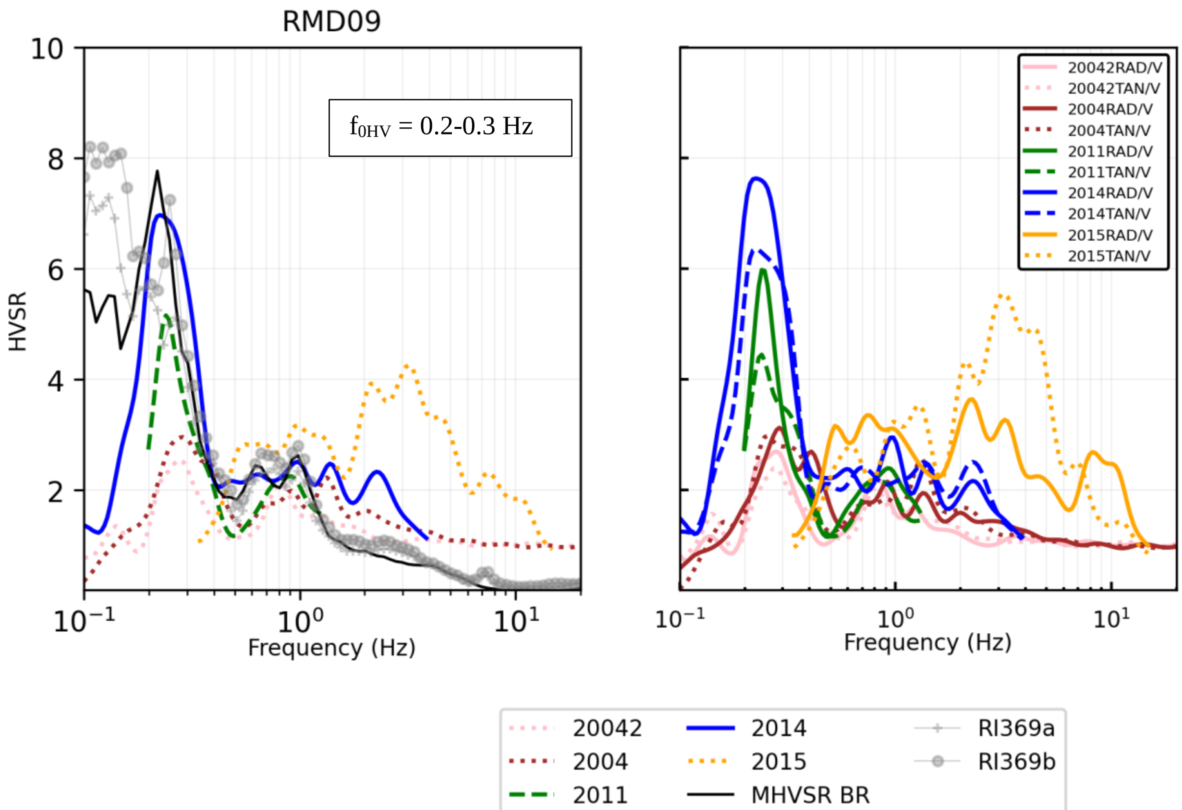
RMD09
f_{0HV} = 0.2-0.3 Hz
HVSR
Frequency (Hz)
20042RAD/V
20042TAN/V
2004RAD/V
2004TAN/V
2011RAD/V
2011TAN/V
2014RAD/V
2014TAN/V
2015RAD/V
2015TAN/V
20042
2004
2011
2014
2015
MHVSR BR
RI369a
RI369b

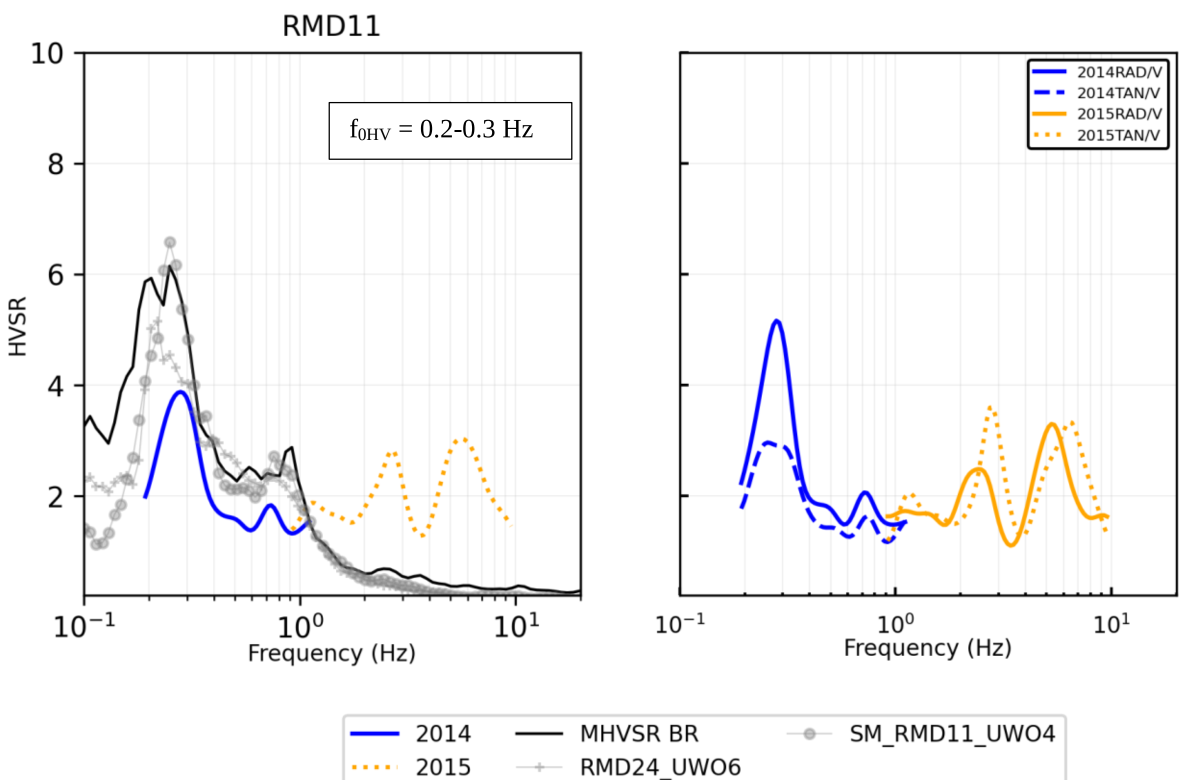
RMD11
f_{0HV} = 0.2-0.3 Hz
HVSR
Frequency (Hz)
2014RAD/V
2014TAN/V
2015RAD/V
2015TAN/V
2014
2015
MHVSR BR
RMD24_UWO6
SM_RMD11_UWO4

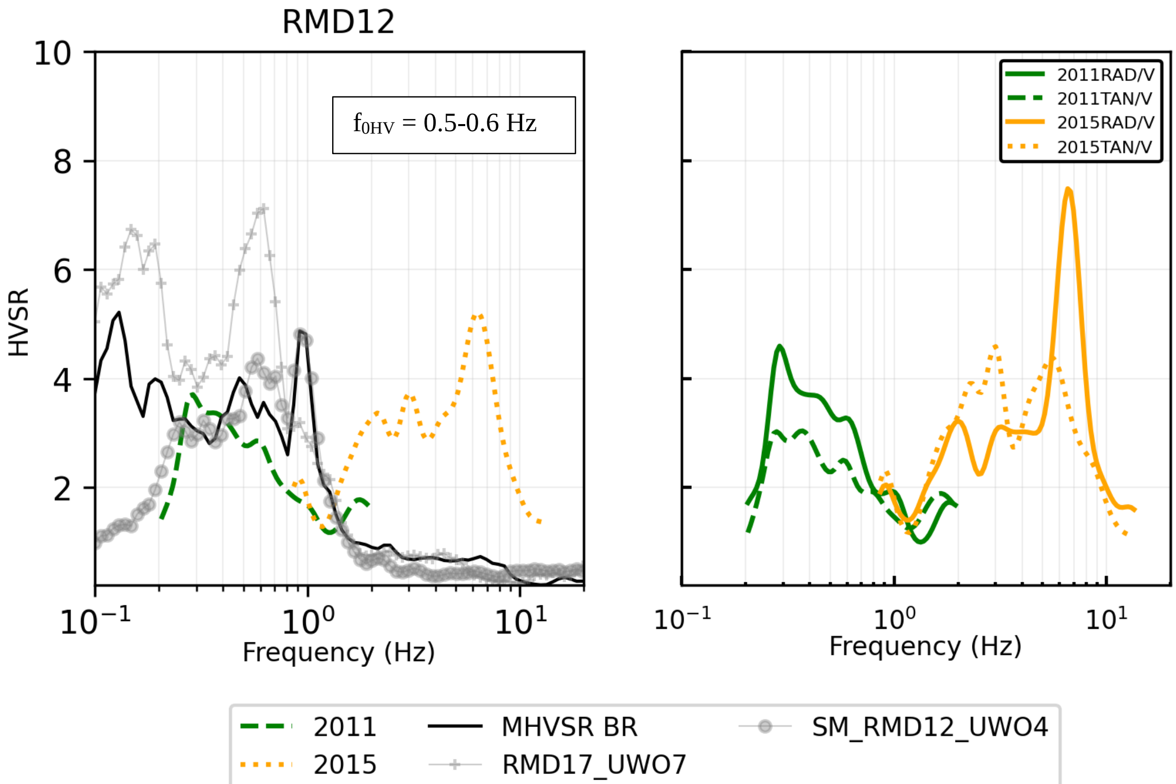
RMD12
HVSR
Frequency (Hz)
f0HV = 0.5-0.6 Hz
2011RAD/V
2011TAN/V
2015RAD/V
2015TAN/V
2011
2015
MHVSR BR
RMD17_UWO7
SM_RMD12_UWO4

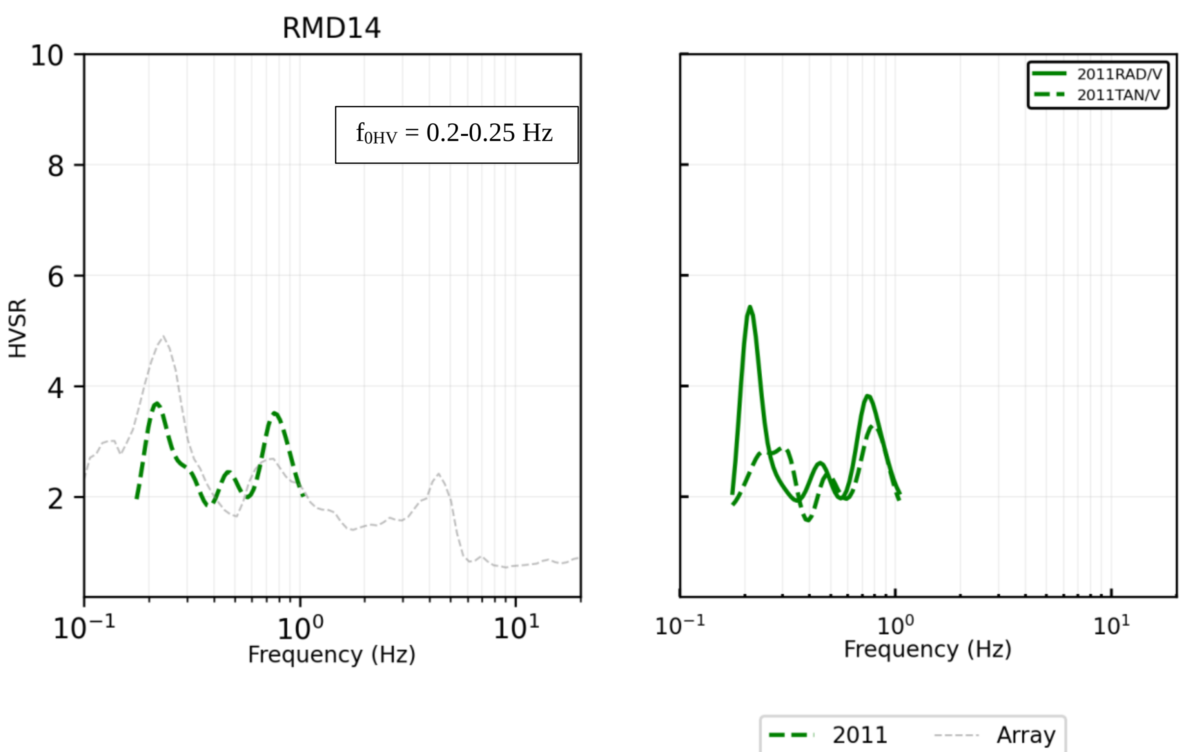
RMD14
HVSR
Frequency (Hz)
f0HV = 0.2-0.25 Hz
2011RAD/V
2011TAN/V
2011
Array

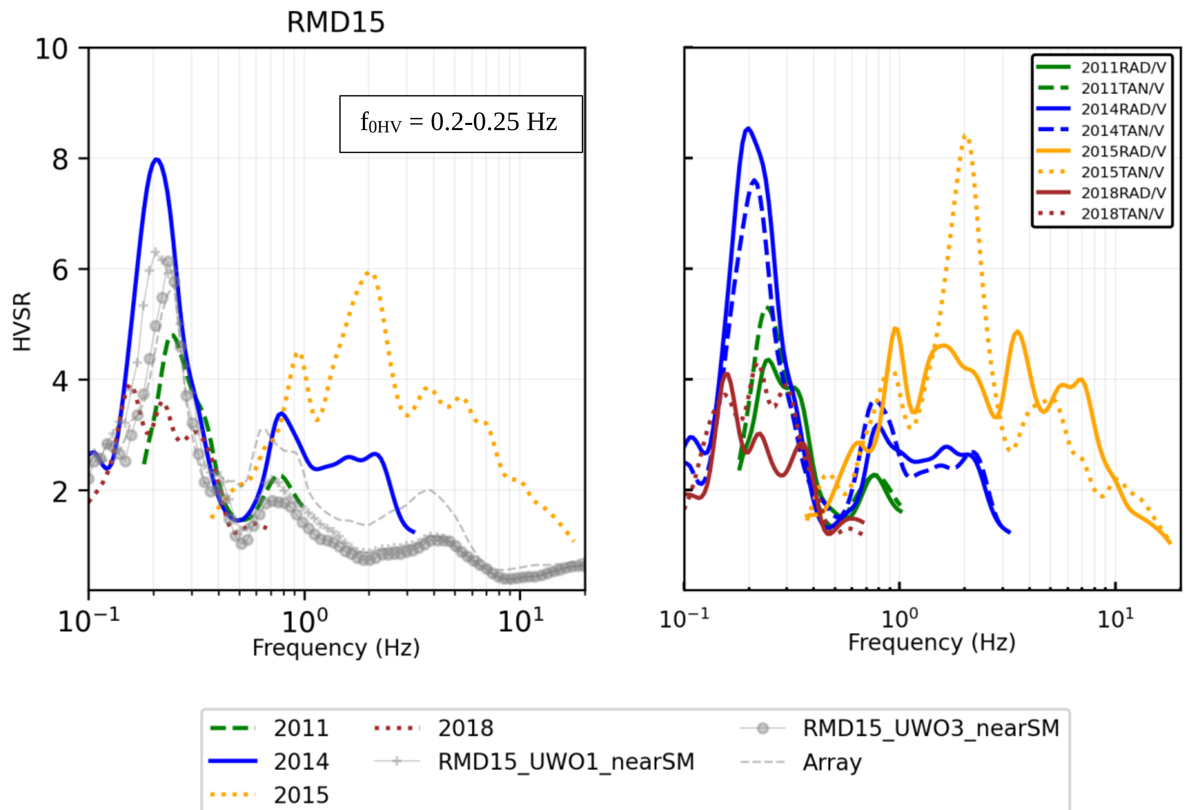

RMD15
f0HV = 0.2-0.25 Hz
HVSR
Frequency (Hz)
2011RAD/V
2011TAN/V
2014RAD/V
2014TAN/V
2015RAD/V
2015TAN/V
2018RAD/V
2018TAN/V
2011
2014
2015
2018
RMD15_UWO1_nearSM
RMD15_UWO3_nearSM
Array

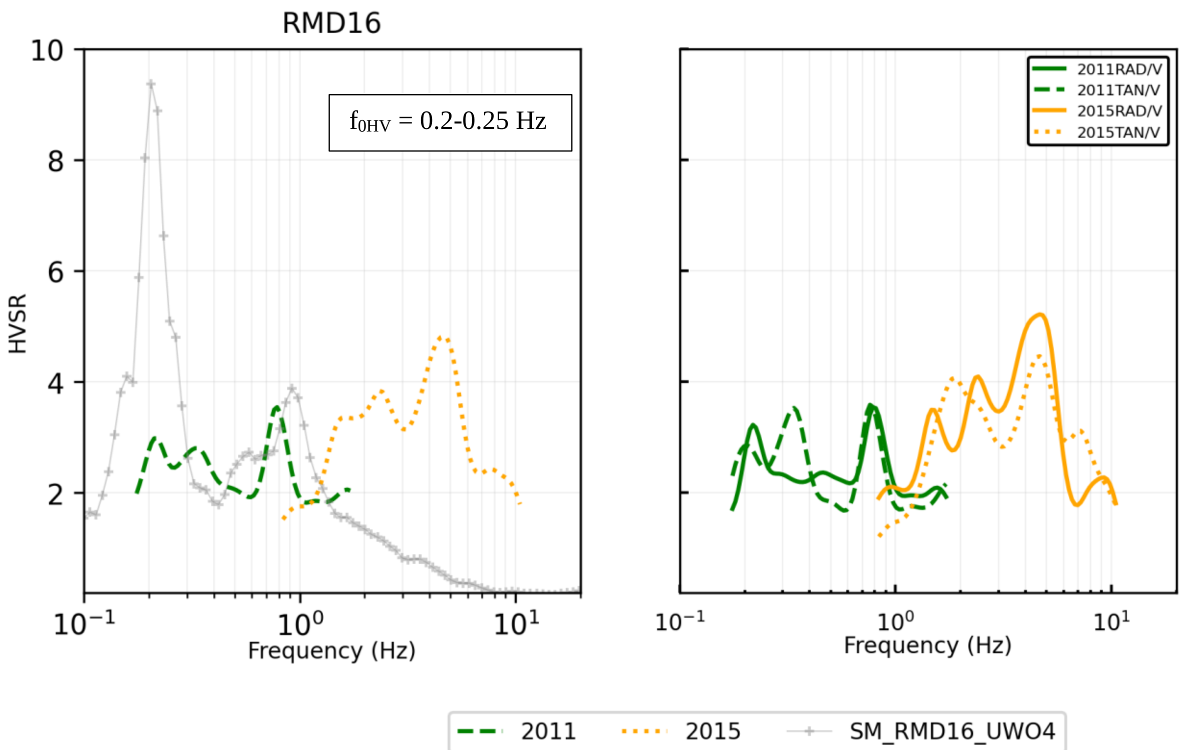

RMD16
f0HV = 0.2-0.25 Hz
HVSR
Frequency (Hz)
2011RAD/V
2011TAN/V
2015RAD/V
2015TAN/V
2011
2015
SM_RMD16_UWO4

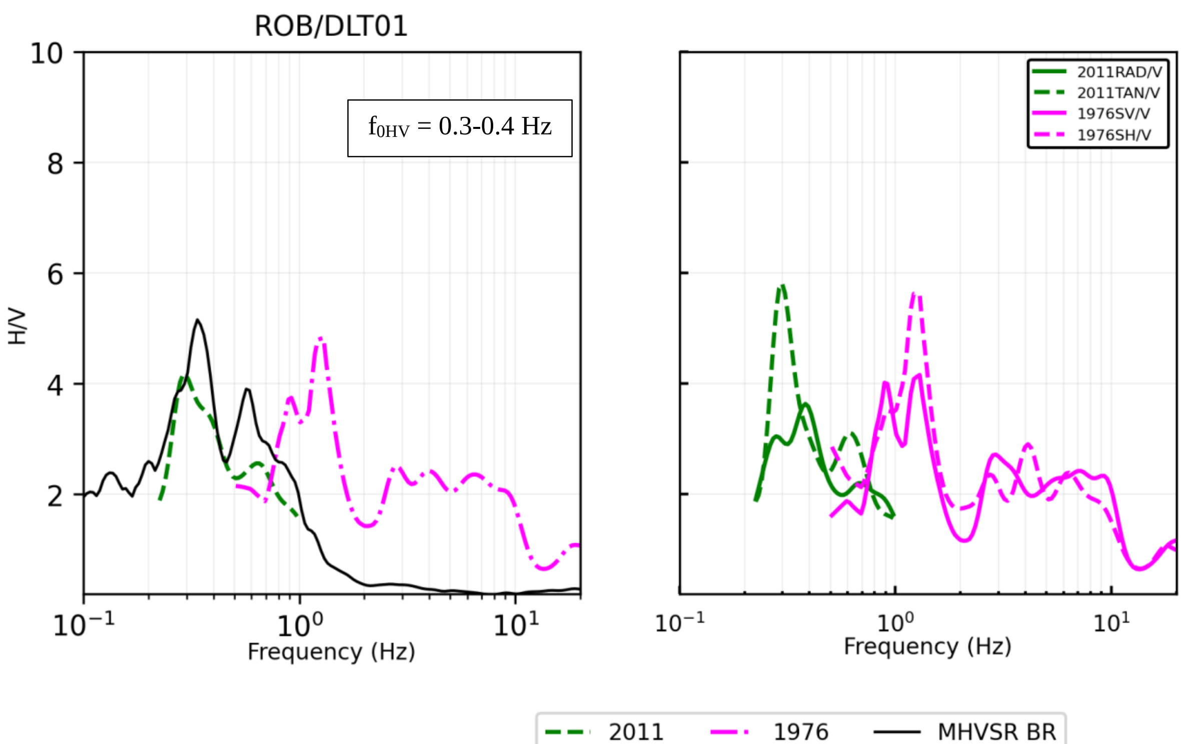

ROB/DLT01
f0HV = 0.3-0.4 Hz
H/V
Frequency (Hz)
2011RAD/V
2011TAN/V
1976SV/V
1976SH/V
2011
1976
MHVSR BR

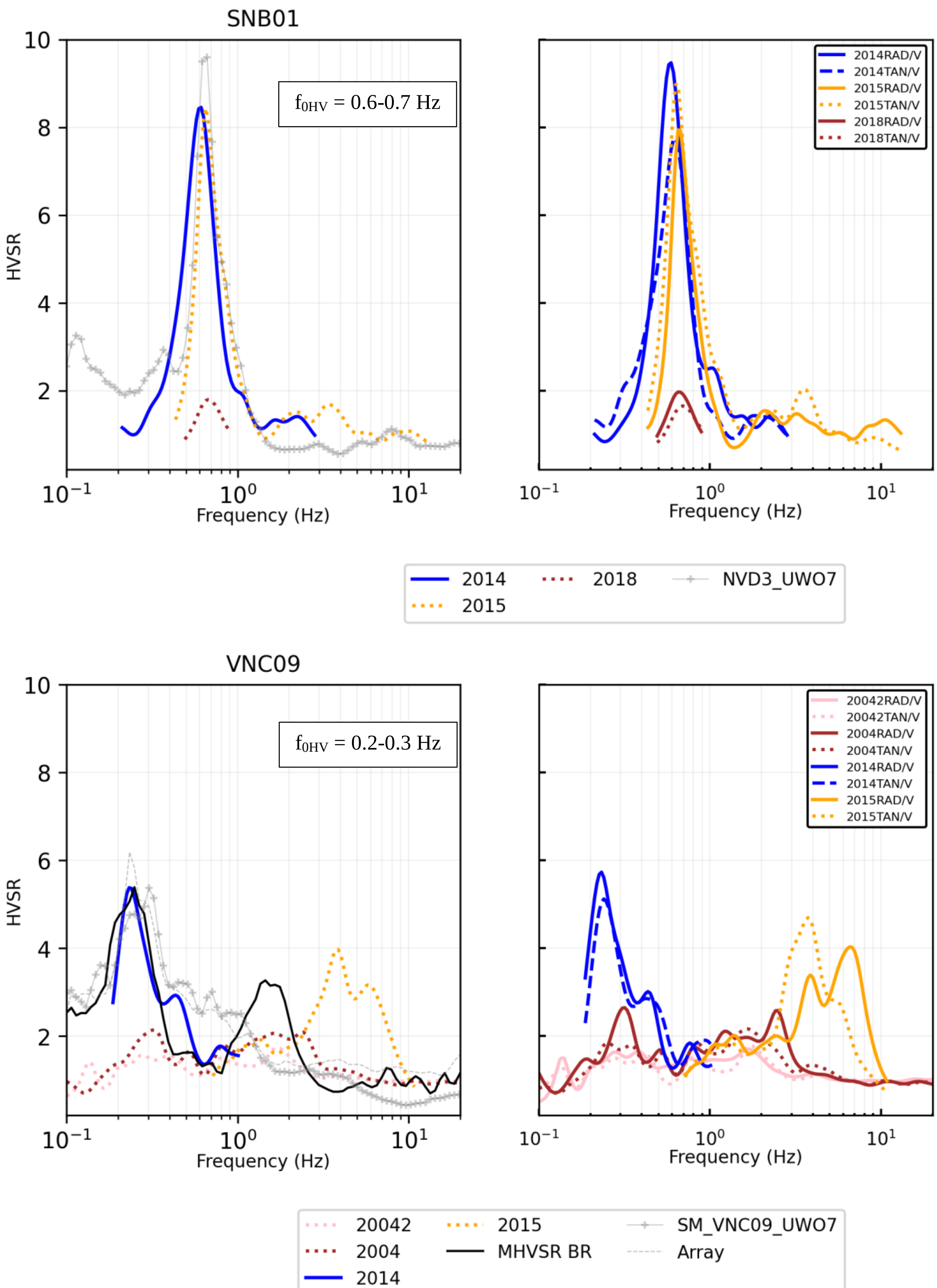

SNB01
f0HV = 0.6-0.7 Hz
HVSR
Frequency (Hz)
2014RAD/V
2014TAN/V
2015RAD/V
2015TAN/V
2018RAD/V
2018TAN/V
2014
2015
2018
NVD3_UWO7
VNC09
f0HV = 0.2-0.3 Hz
HVSR
Frequency (Hz)
20042RAD/V
20042TAN/V
2004RAD/V
2004TAN/V
2014RAD/V
2014TAN/V
2015RAD/V
2015TAN/V
20042
2004
2014
2015
MHVSR BR
SM_VNC09_UWO7
Array

Stiff Sites

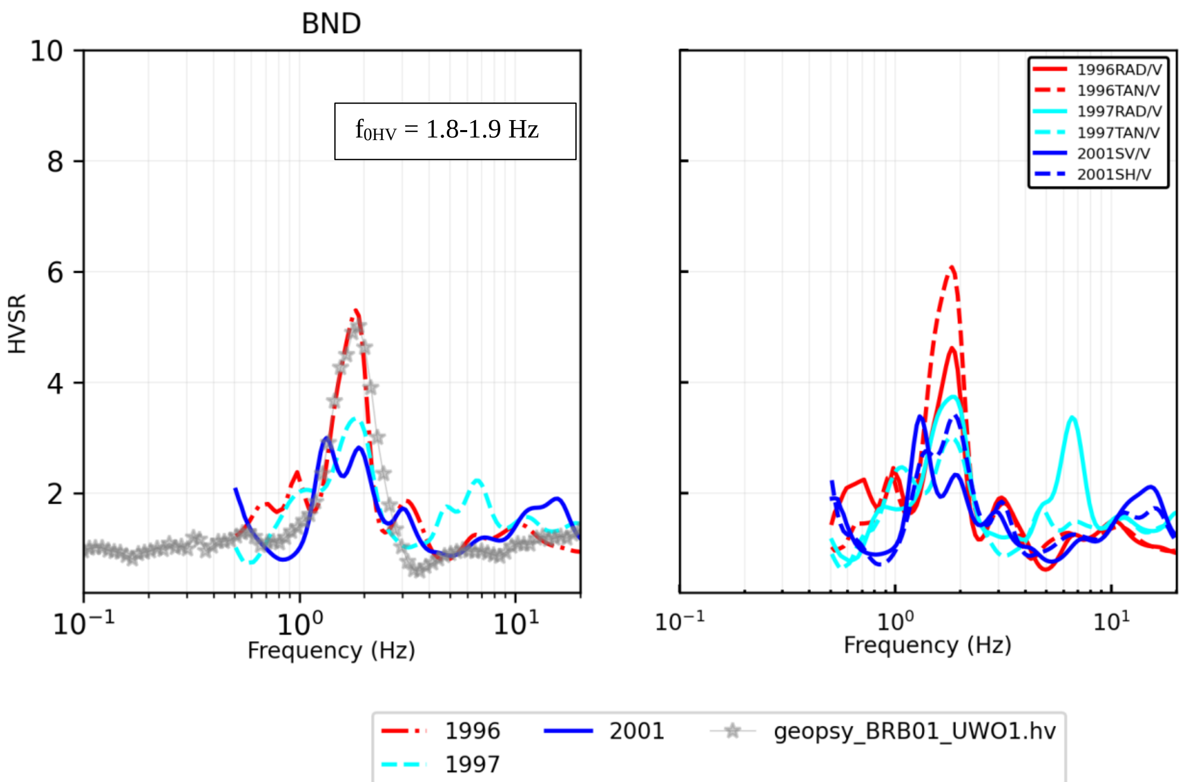
BND
f_{0HV} = 1.8-1.9 Hz
HVSR
Frequency (Hz)
1996RAD/V
1996TAN/V
1997RAD/V
1997TAN/V
2001SV/V
2001SH/V
1996
2001
geopsy_BRB01_UWO1.hv
1997

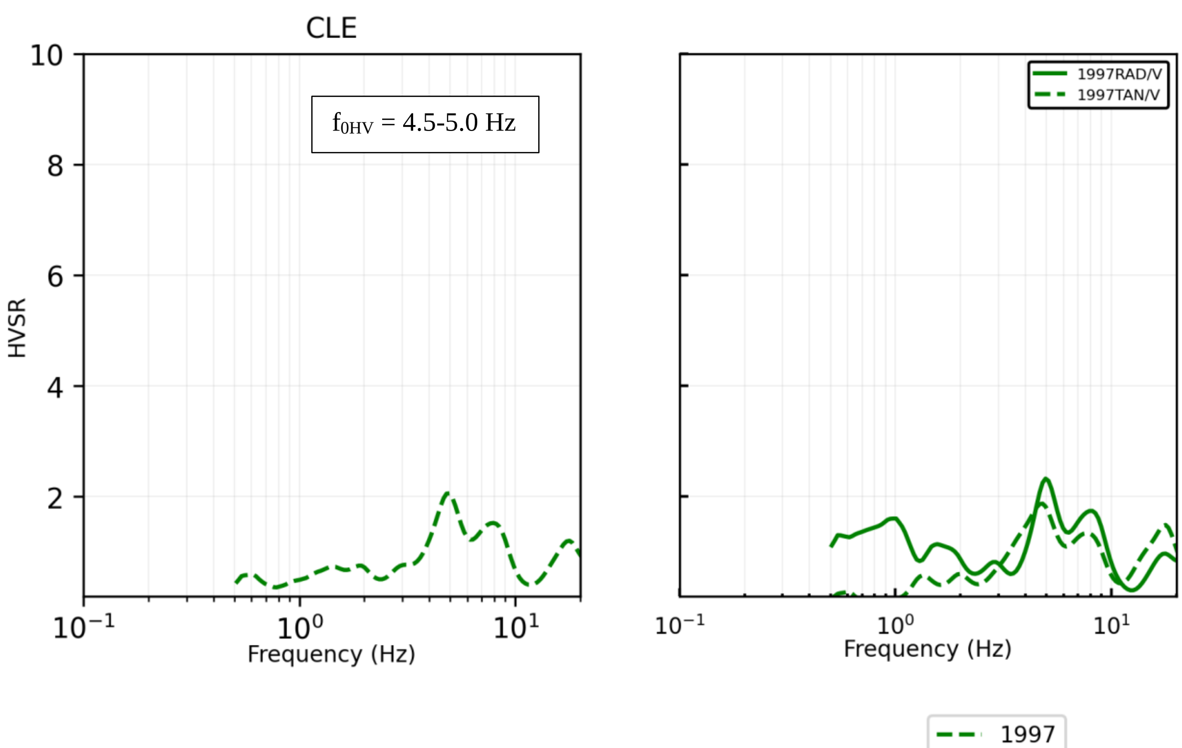
CLE
f_{0HV} = 4.5-5.0 Hz
HVSR
Frequency (Hz)
1997RAD/V
1997TAN/V
1997

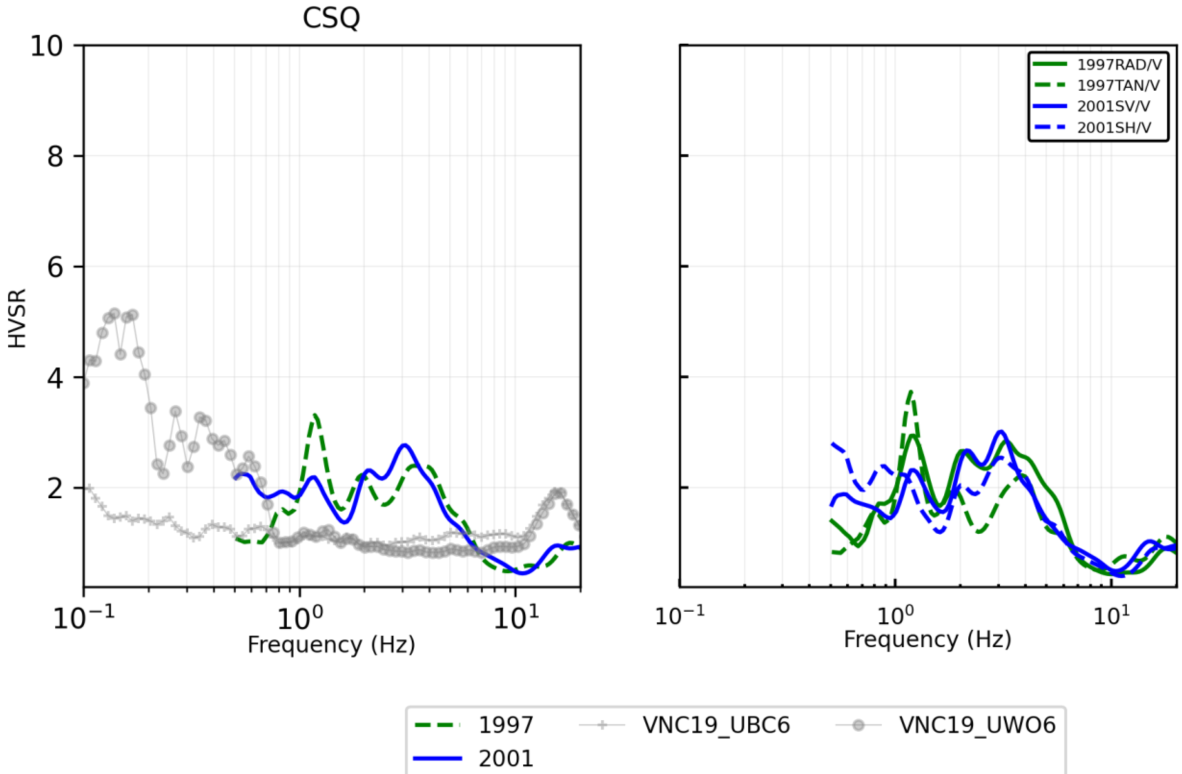
CSQ
HVSR
Frequency (Hz)
1997RAD/V
1997TAN/V
2001SV/V
2001SH/V
1997
2001
VNC19_UBC6
VNC19_UWO6

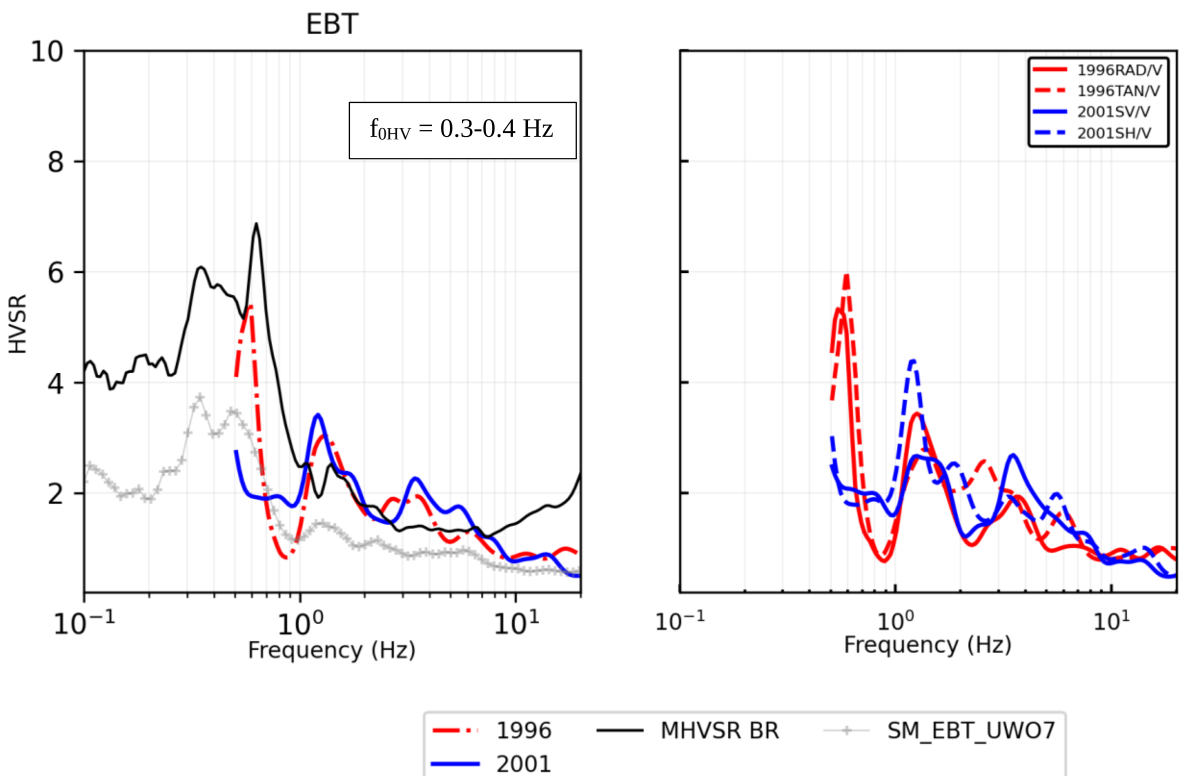
EBT
HVSR
f_{0HV} = 0.3-0.4 Hz
Frequency (Hz)
1996RAD/V
1996TAN/V
2001SV/V
2001SH/V
1996
2001
MHVSR BR
SM_EBT_UWO7

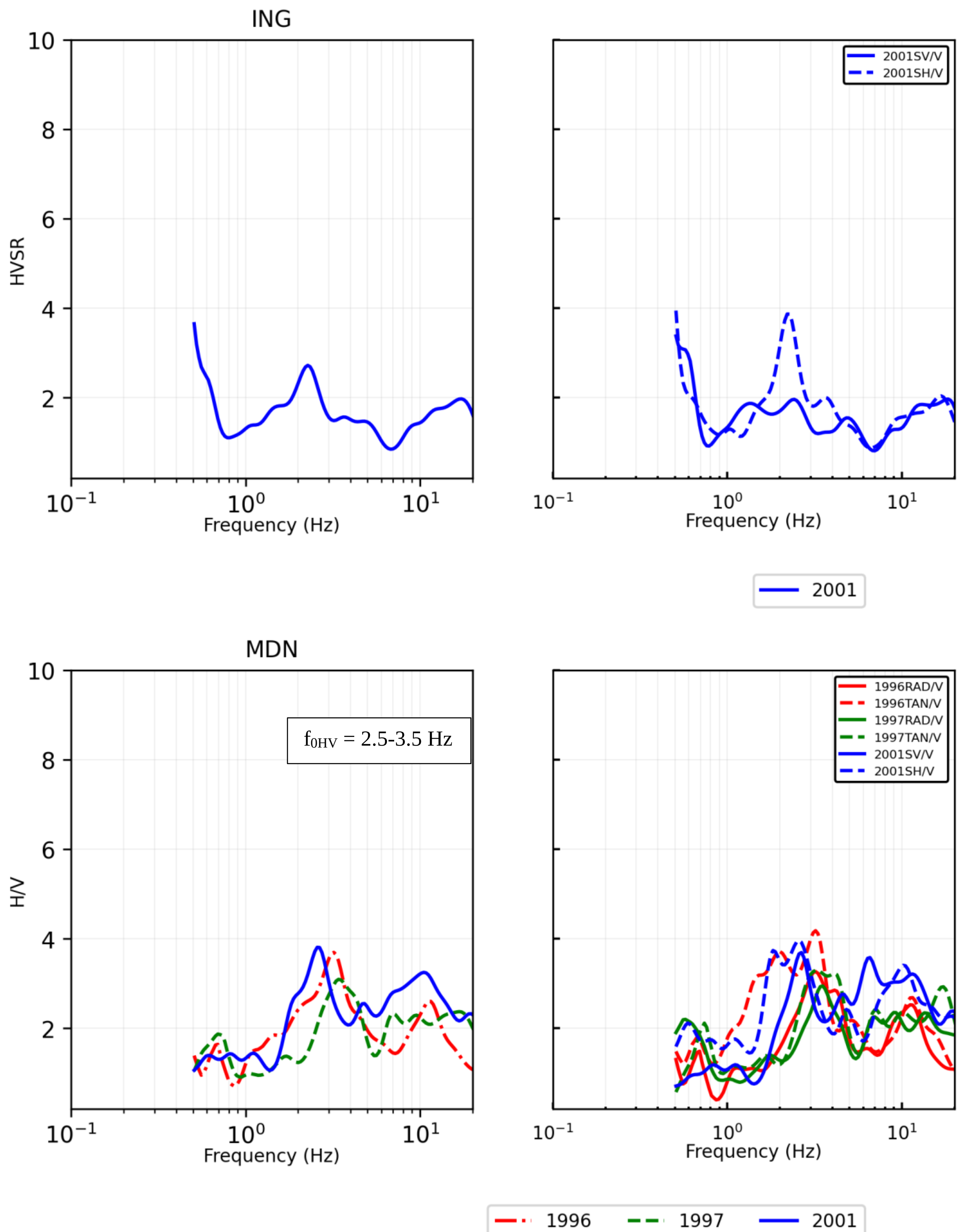

ING
HVSR
Frequency (Hz)
2001SV/V
2001SH/V
2001
MDN
H/V
f0HV = 2.5-3.5 Hz
1996RAD/V
1996TAN/V
1997RAD/V
1997TAN/V
2001SV/V
2001SH/V
1996
1997
2001

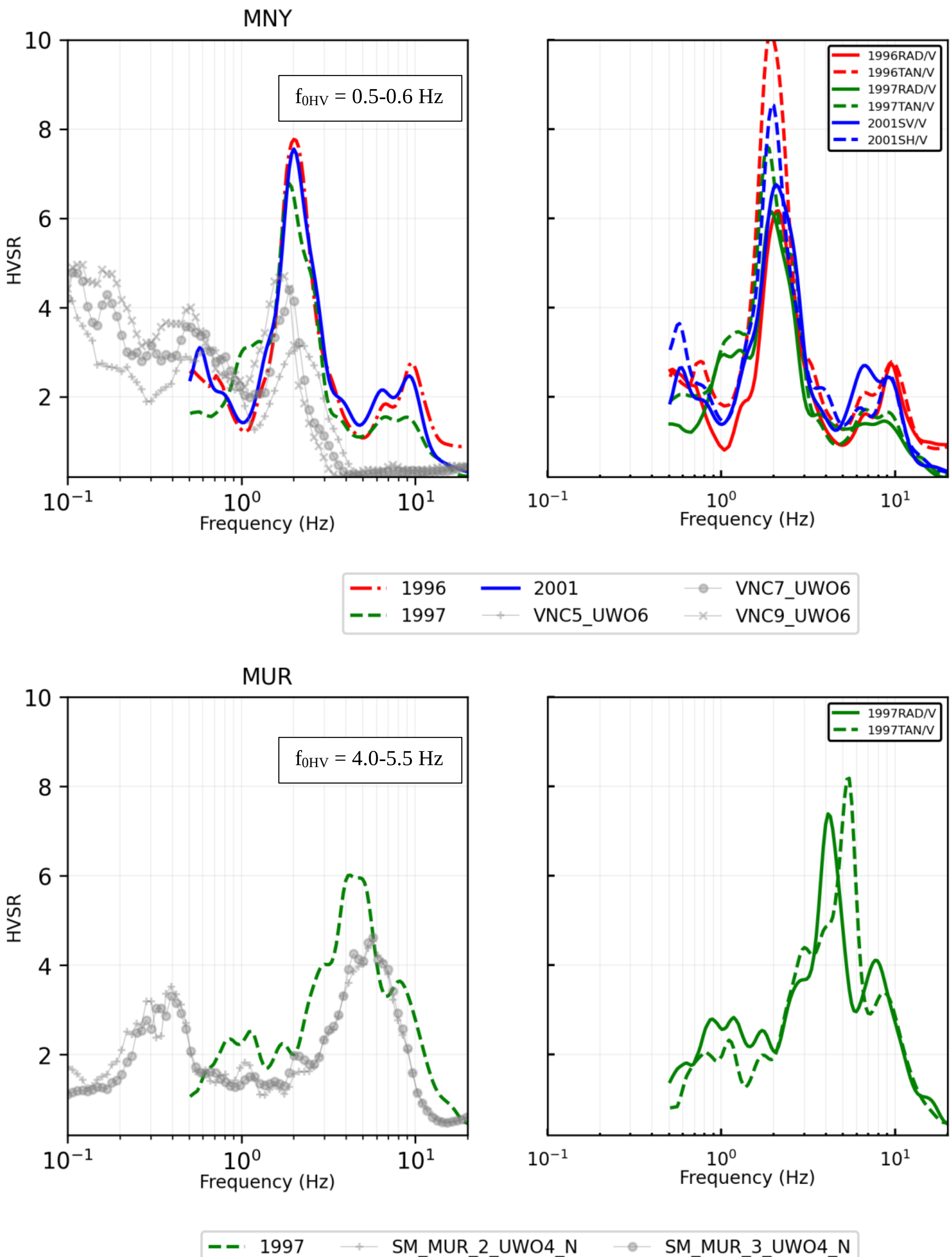
MNY
f_{0HV} = 0.5-0.6 Hz
HVSR
Frequency (Hz)
1996RAD/V
1996TAN/V
1997RAD/V
1997TAN/V
2001SV/V
2001SH/V
1996
1997
2001
VNC5_UWO6
VNC7_UWO6
VNC9_UWO6
MUR
f_{0HV} = 4.0-5.5 Hz
1997RAD/V
1997TAN/V
1997
SM_MUR_2_UWO4_N
SM_MUR_3_UWO4_N

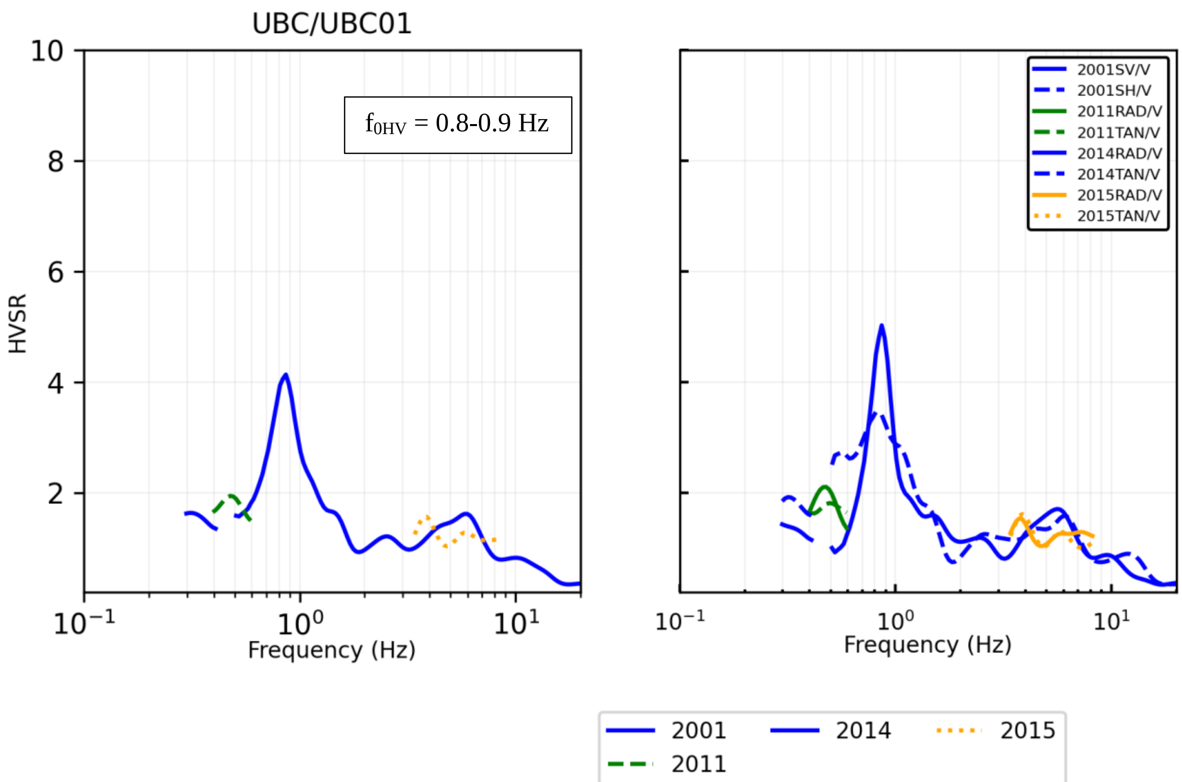
UBC/UBC01
f_{0HV} = 0.8-0.9 Hz
HVSR
Frequency (Hz)
2001SV/V
2001SH/V
2011RAD/V
2011TAN/V
2014RAD/V
2014TAN/V
2015RAD/V
2015TAN/V
2001
2014
2015
2011

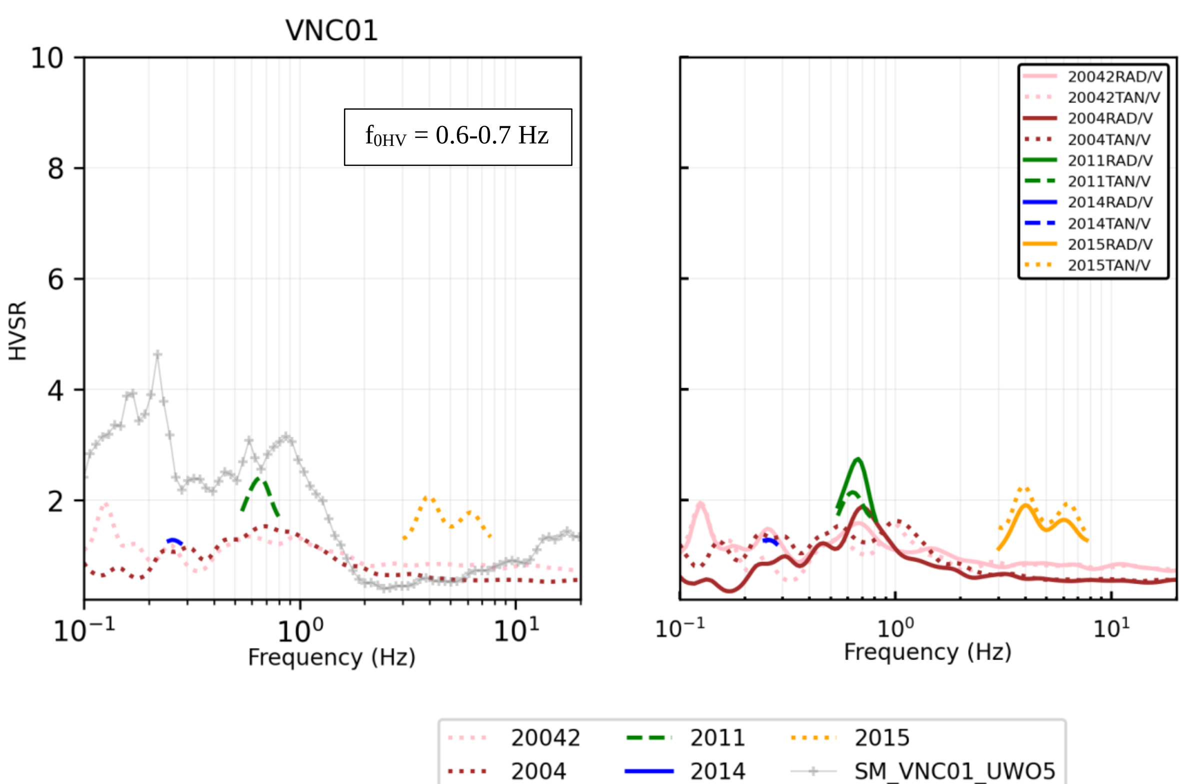
VNC01
f_{0HV} = 0.6-0.7 Hz
HVSR
Frequency (Hz)
20042RAD/V
20042TAN/V
2004RAD/V
2004TAN/V
2011RAD/V
2011TAN/V
2014RAD/V
2014TAN/V
2015RAD/V
2015TAN/V
20042
2011
2015
2004
2014
SM_VNC01_UWO5

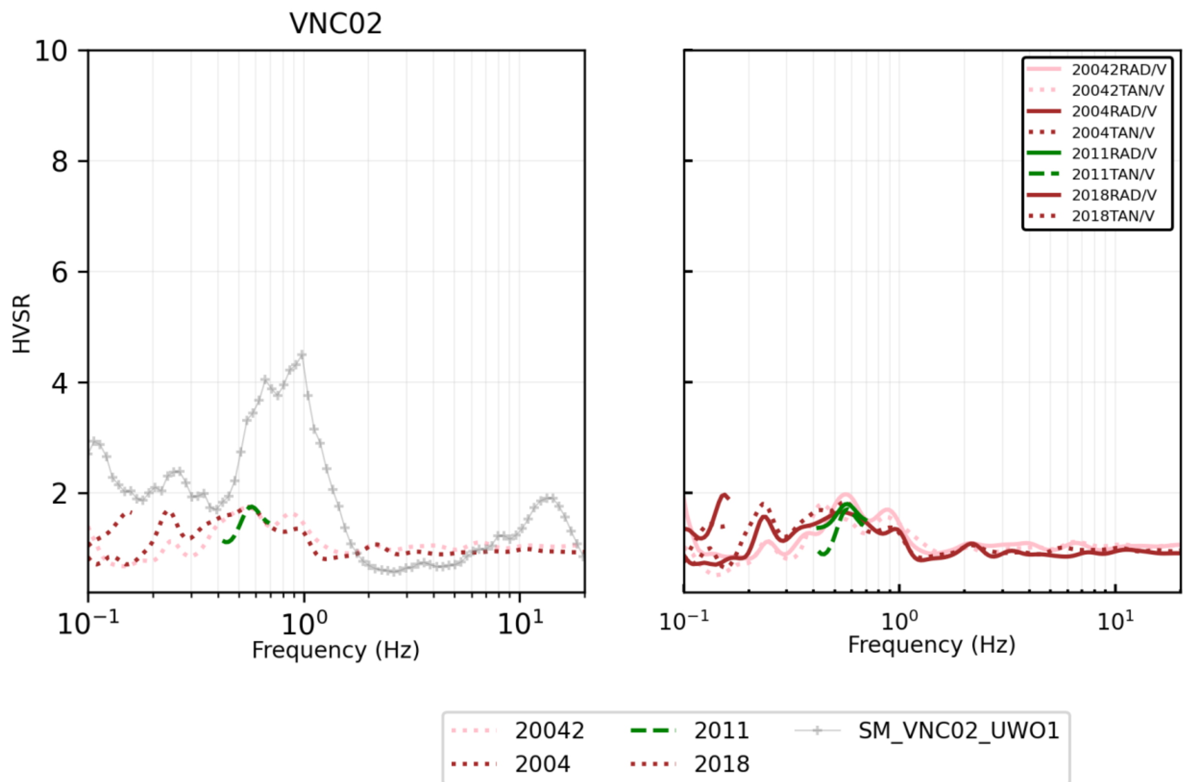
VNC02
HVSR
Frequency (Hz)
20042RAD/V
20042TAN/V
2004RAD/V
2004TAN/V
2011RAD/V
2011TAN/V
2018RAD/V
2018TAN/V
20042
2004
2011
2018
SM_VNC02_UWO1

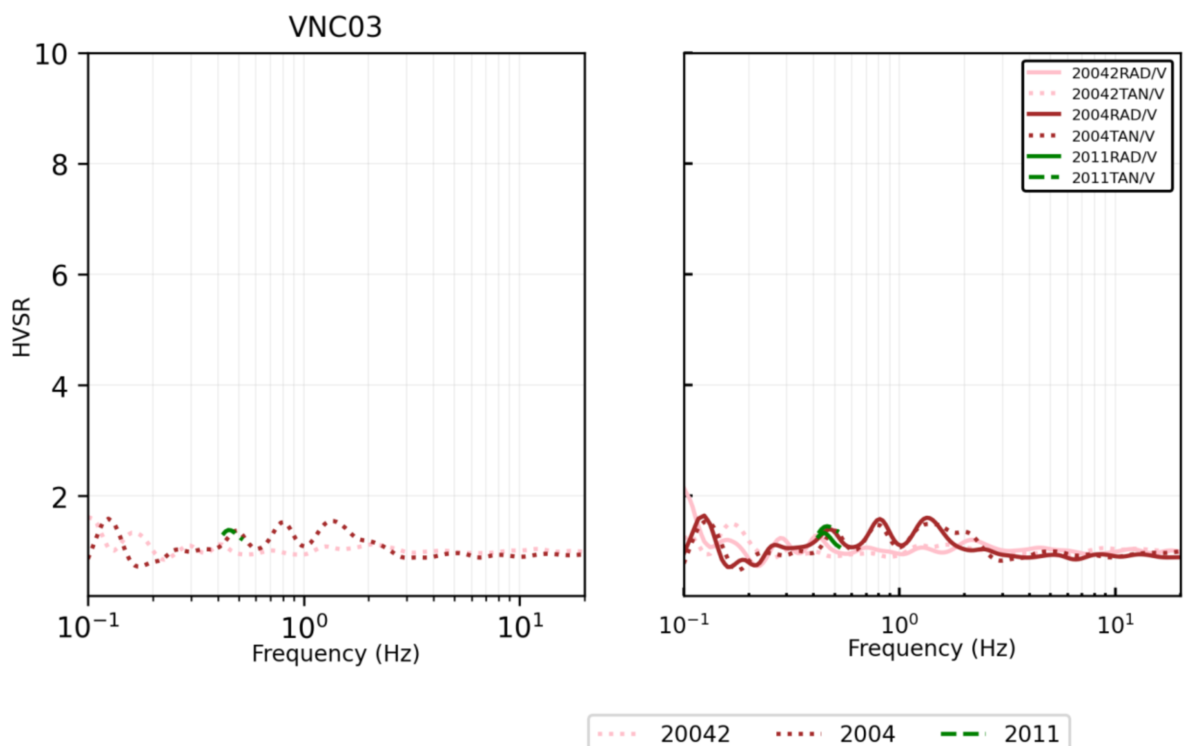
VNC03
HVSR
Frequency (Hz)
20042RAD/V
20042TAN/V
2004RAD/V
2004TAN/V
2011RAD/V
2011TAN/V
20042
2004
2011

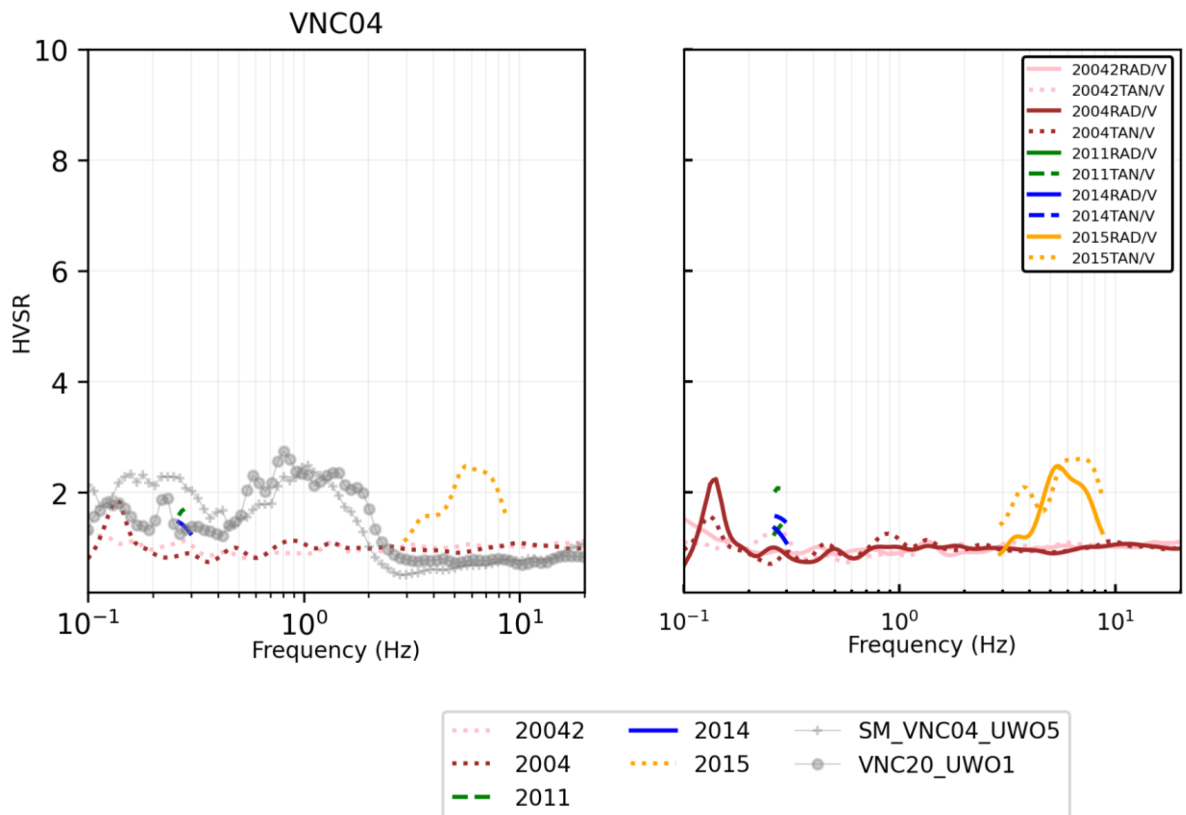
VNC04
HVSR
Frequency (Hz)
20042RAD/V
20042TAN/V
2004RAD/V
2004TAN/V
2011RAD/V
2011TAN/V
2014RAD/V
2014TAN/V
2015RAD/V
2015TAN/V
20042
2004
2011
2014
2015
SM_VNC04_UWO5
VNC20_UWO1

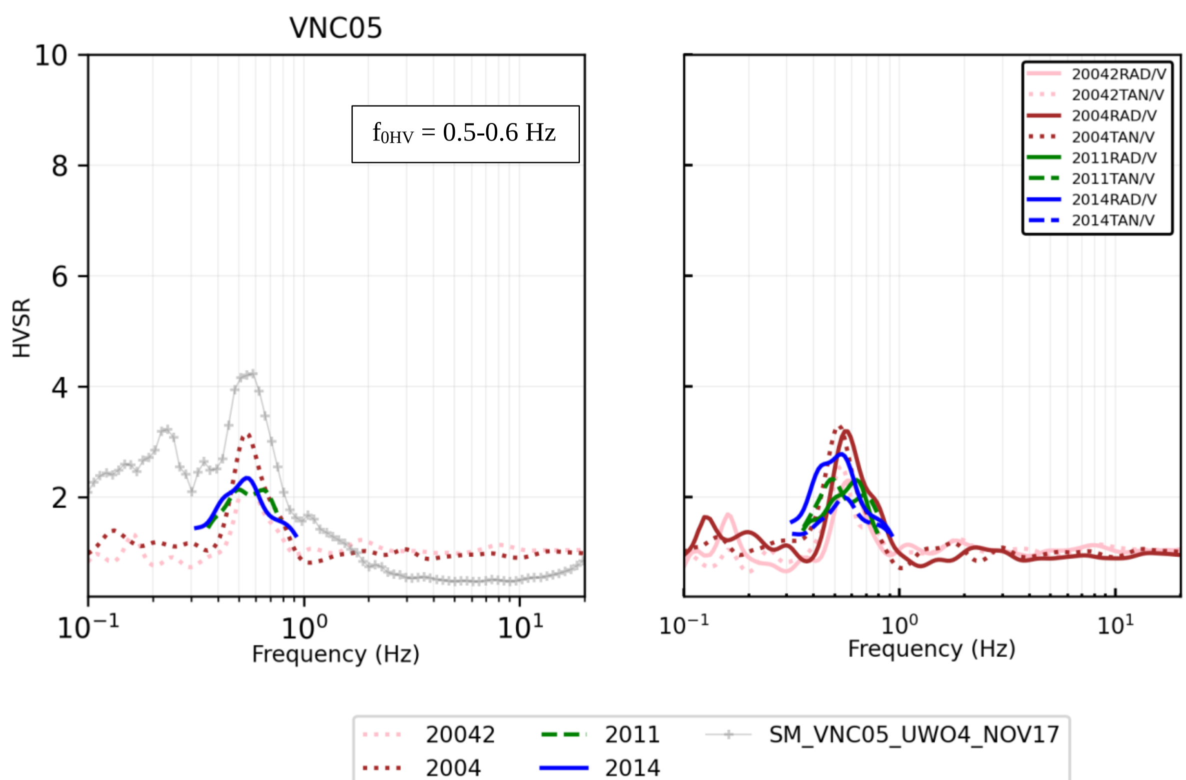
VNC05
HVSR
f_{0HV} = 0.5-0.6 Hz
Frequency (Hz)
20042RAD/V
20042TAN/V
2004RAD/V
2004TAN/V
2011RAD/V
2011TAN/V
2014RAD/V
2014TAN/V
20042
2004
2011
2014
SM_VNC05_UWO4_NOV17

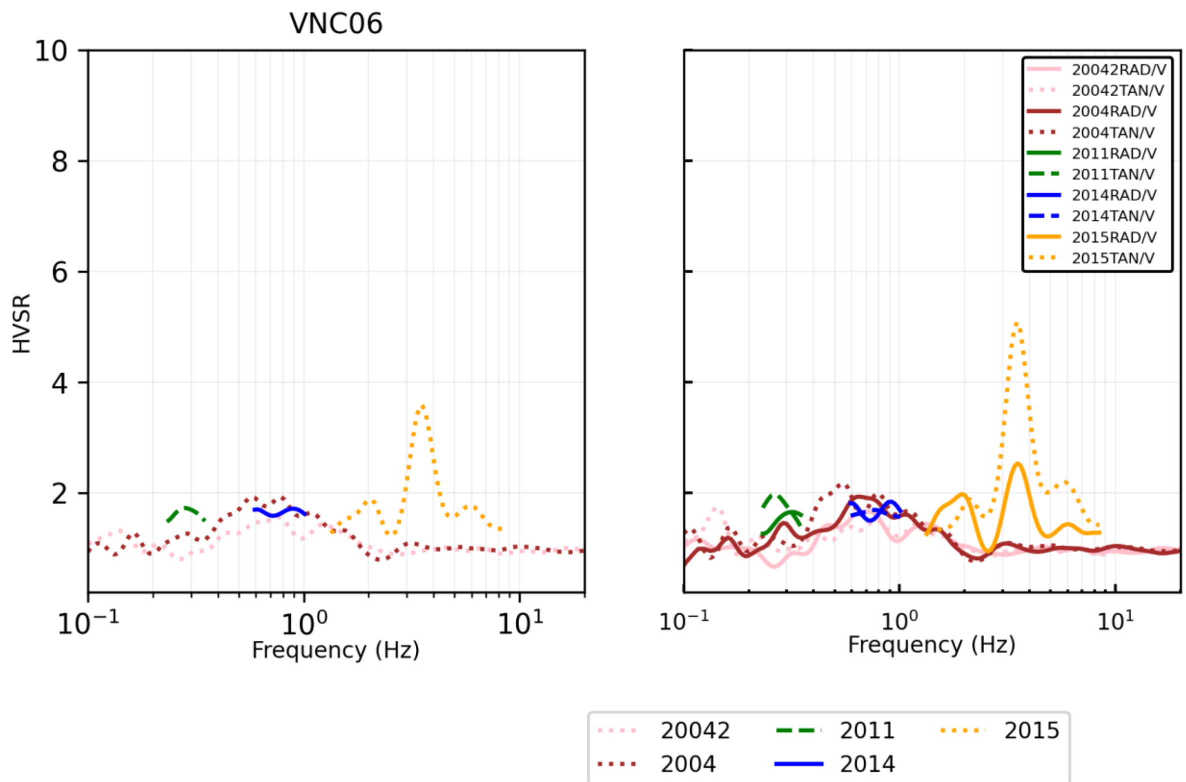
VNC06
HVSR
Frequency (Hz)
20042RAD/V
20042TAN/V
2004RAD/V
2004TAN/V
2011RAD/V
2011TAN/V
2014RAD/V
2014TAN/V
2015RAD/V
2015TAN/V
20042
2004
2011
2014
2015

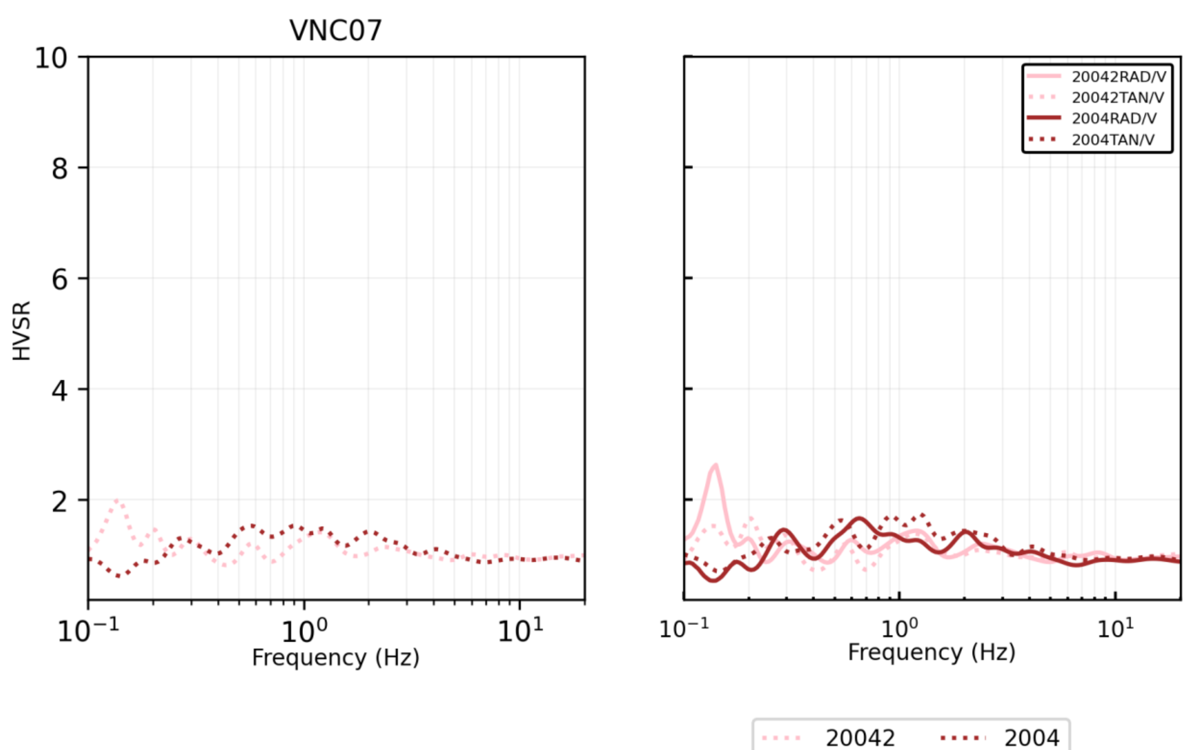
VNC07
HVSR
Frequency (Hz)
20042RAD/V
20042TAN/V
2004RAD/V
2004TAN/V
20042
2004

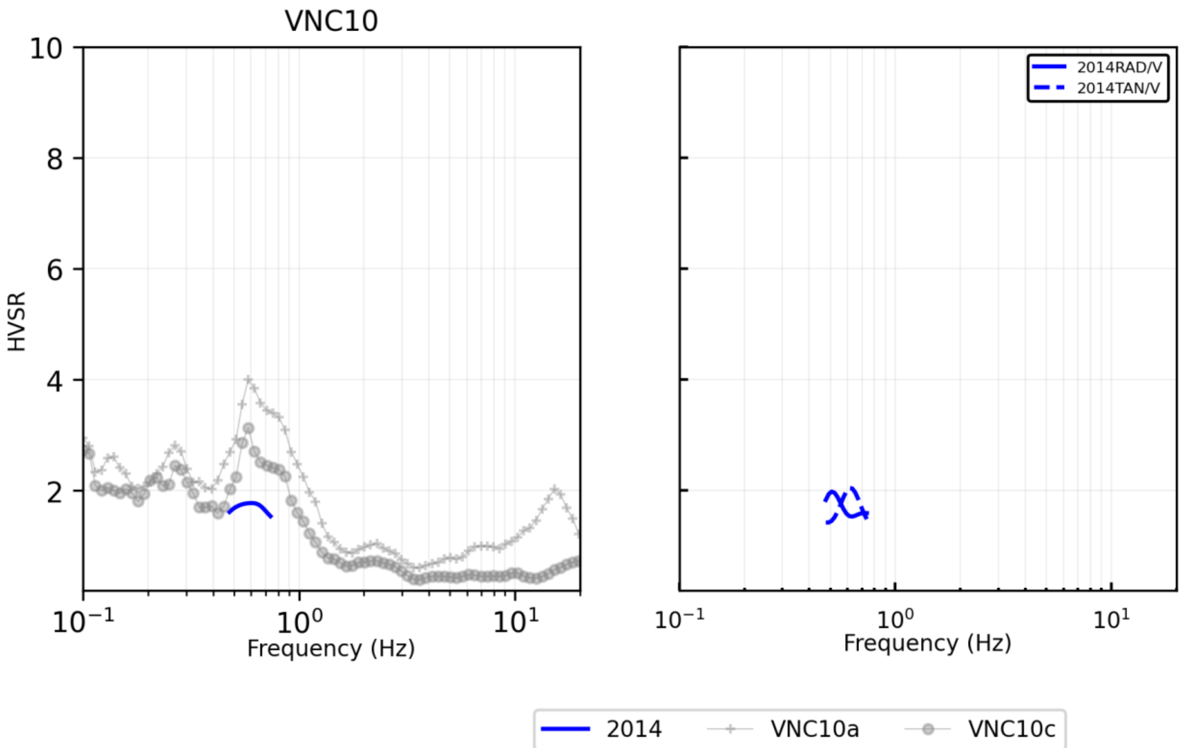
VNC10
HVSR
Frequency (Hz)
2014RAD/V
2014TAN/V
2014
VNC10a
VNC10c

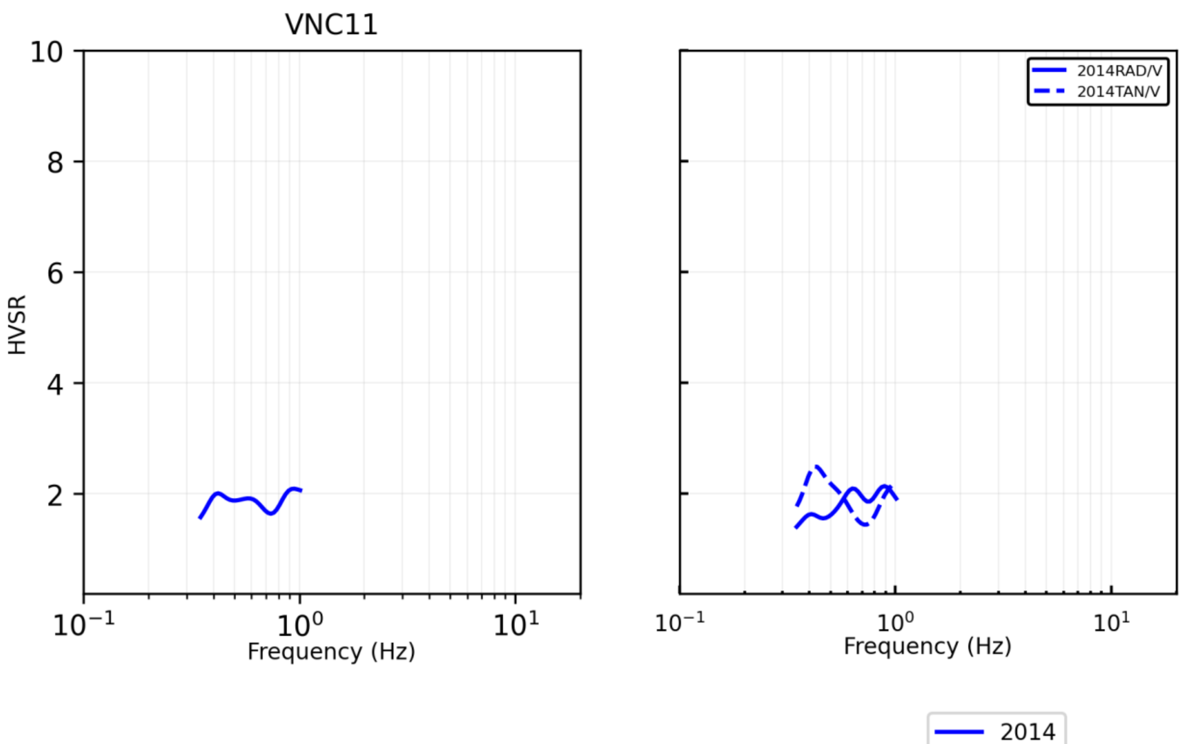
VNC11
HVSR
Frequency (Hz)
2014RAD/V
2014TAN/V
2014

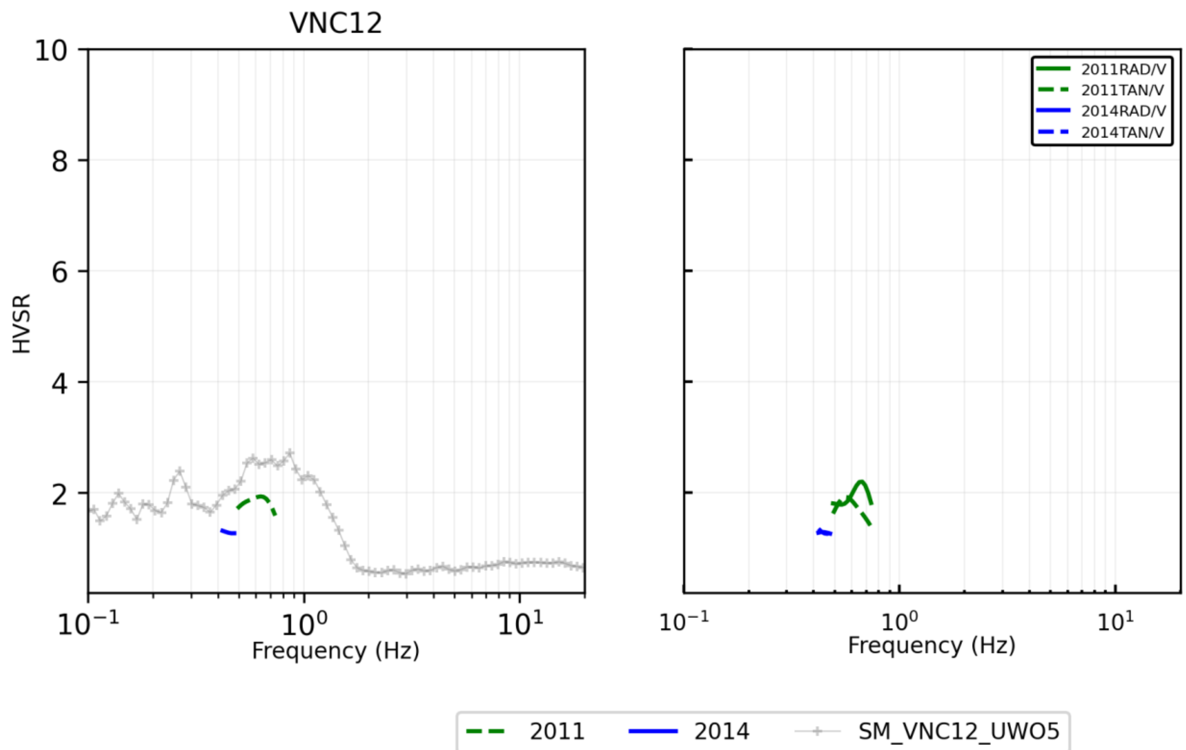

VNC12
10
8
6
4
2
HVSR
10^{-1}
10^{0}
10^{1}
Frequency (Hz)
2011RAD/V
2011TAN/V
2014RAD/V
2014TAN/V
2011
2014
SM_VNC12_UWO5

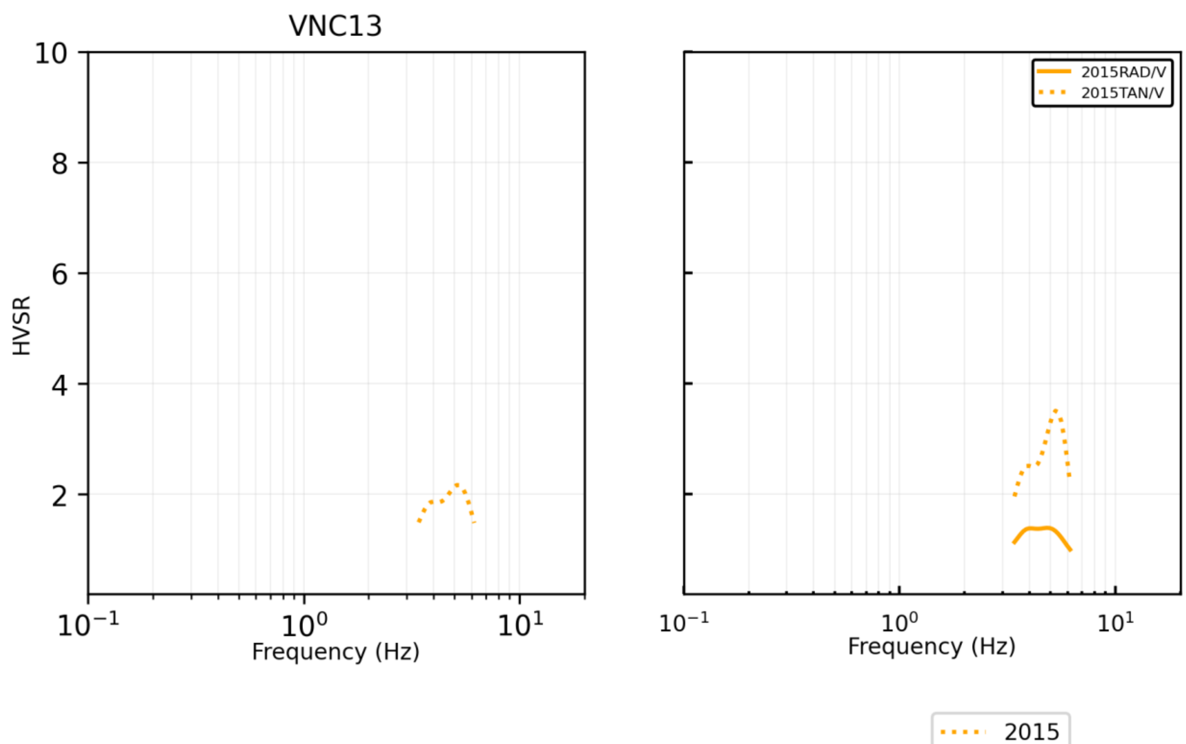

VNC13
10
8
6
4
2
HVSR
10^{-1}
10^{0}
10^{1}
Frequency (Hz)
2015RAD/V
2015TAN/V
2015

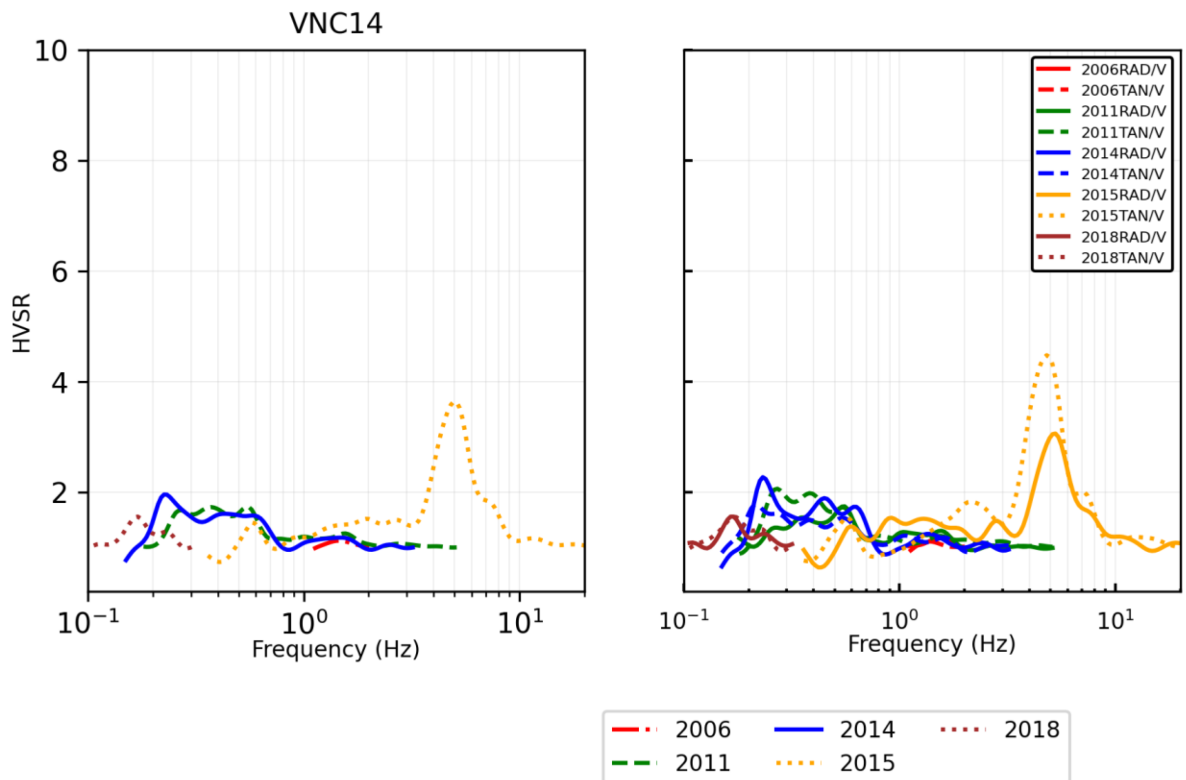
VNC14
10
8
6
4
2
HVSR
10^{-1}
10^{0}
10^{1}
Frequency (Hz)
2006RAD/V
2006TAN/V
2011RAD/V
2011TAN/V
2014RAD/V
2014TAN/V
2015RAD/V
2015TAN/V
2018RAD/V
2018TAN/V
2006
2011
2014
2015
2018

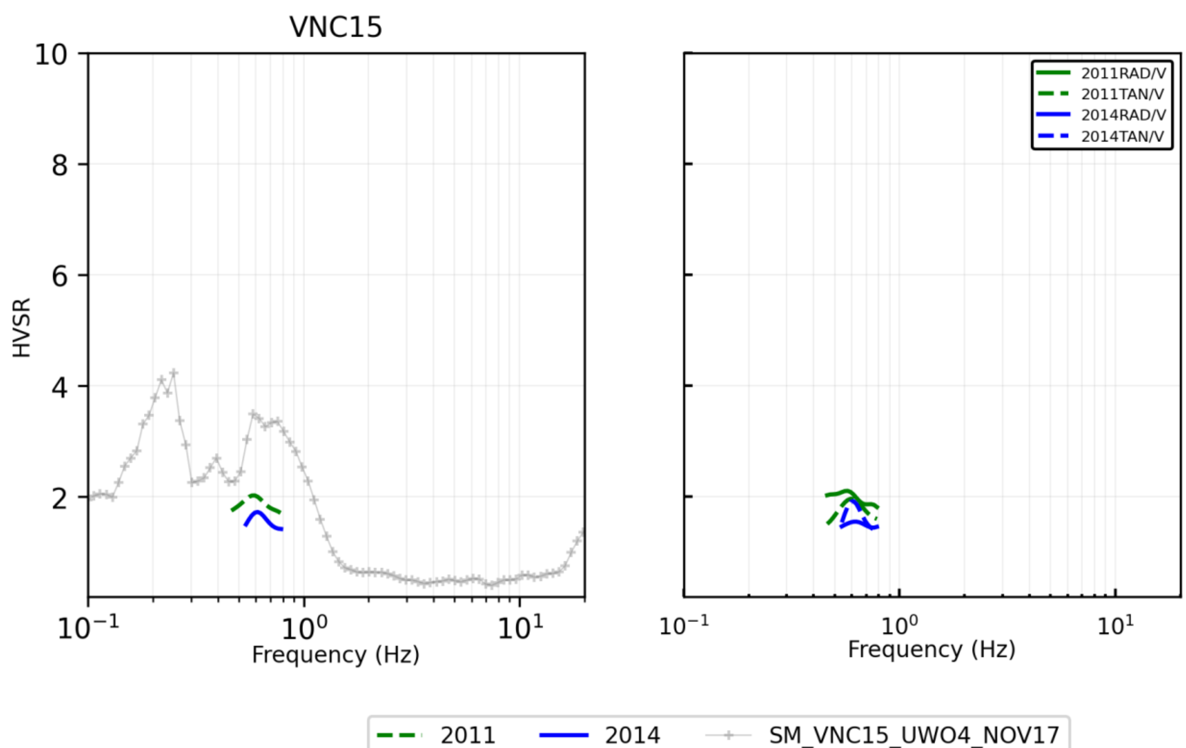
VNC15
10
8
6
4
2
HVSR
10^{-1}
10^{0}
10^{1}
Frequency (Hz)
2011RAD/V
2011TAN/V
2014RAD/V
2014TAN/V
2011
2014
SM_VNC15_UWO4_NOV17

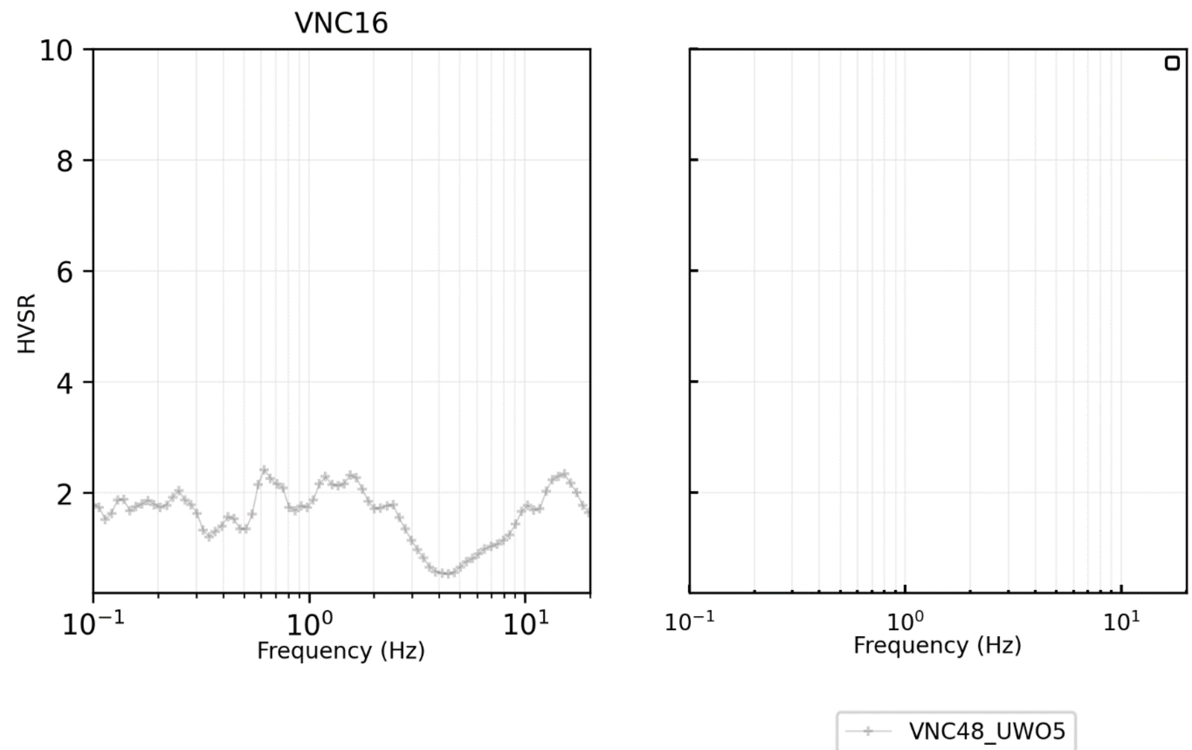
VNC16
HVSR
Frequency (Hz)
Frequency (Hz)
VNC48_UWO5

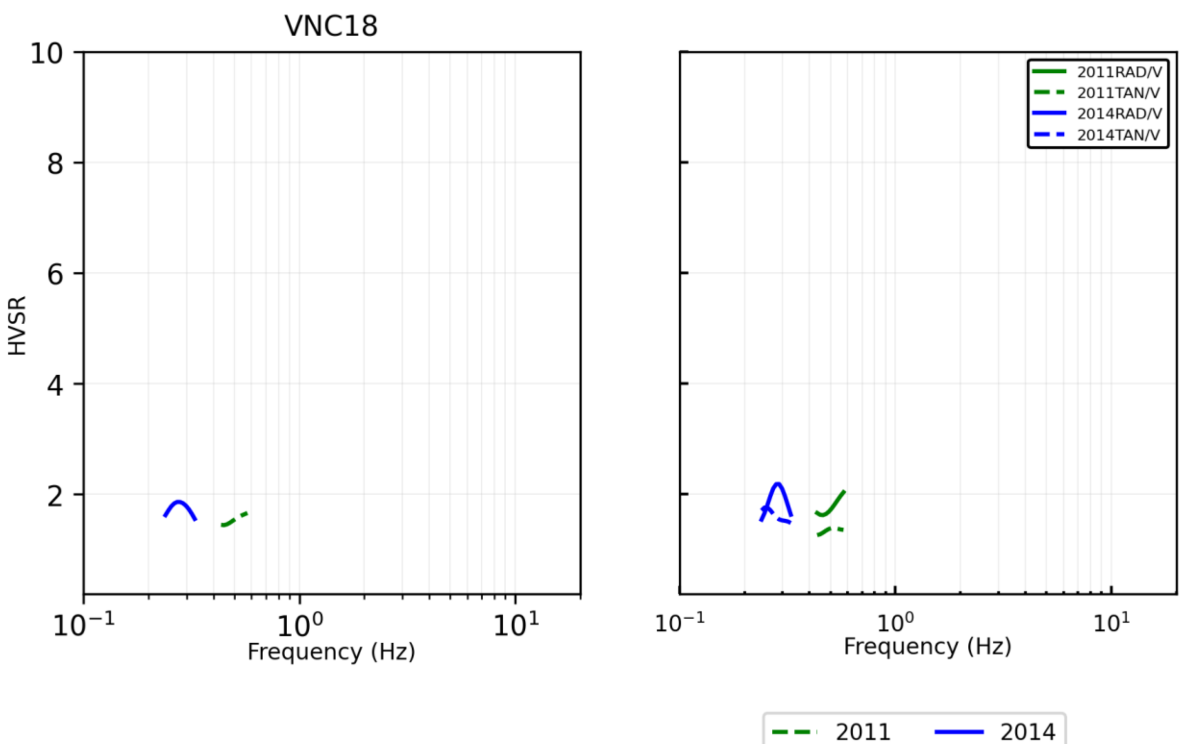
VNC18
HVSR
Frequency (Hz)
Frequency (Hz)
2011RAD/V
2011TAN/V
2014RAD/V
2014TAN/V
2011
2014

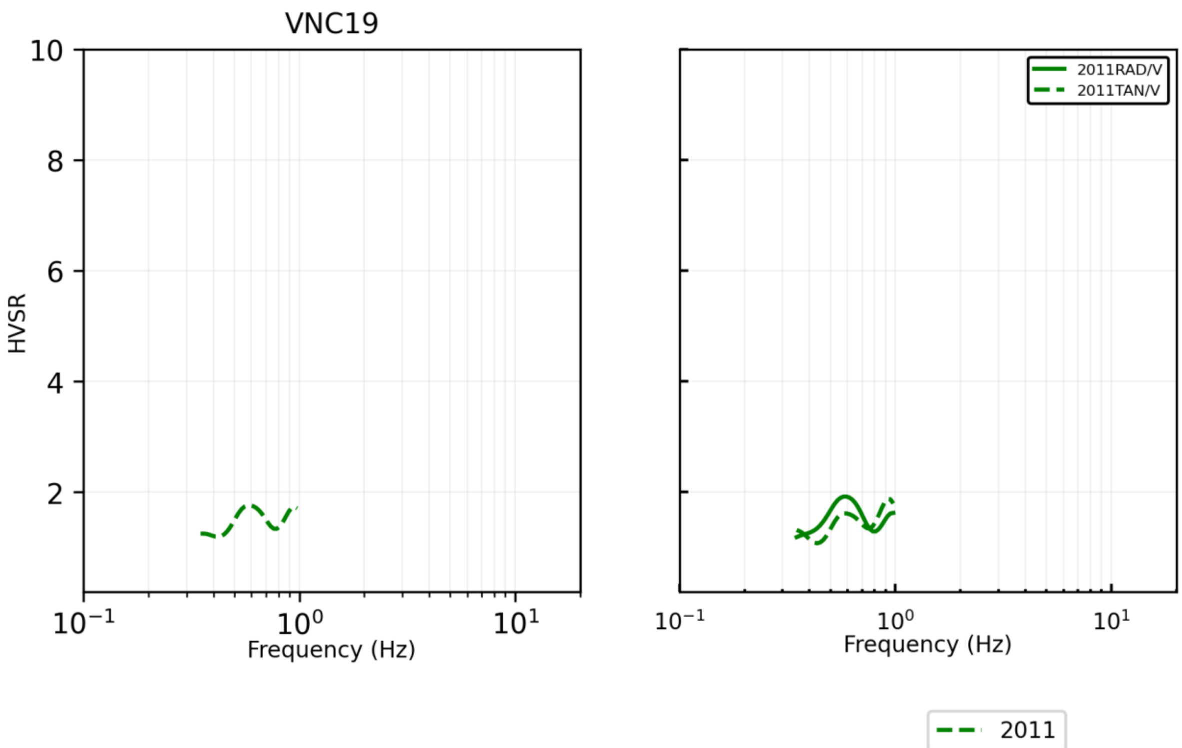
VNC19
10
8
6
4
2
HVSR
10^{-1}
10^{0}
10^{1}
Frequency (Hz)
2011RAD/V
2011TAN/V
2011

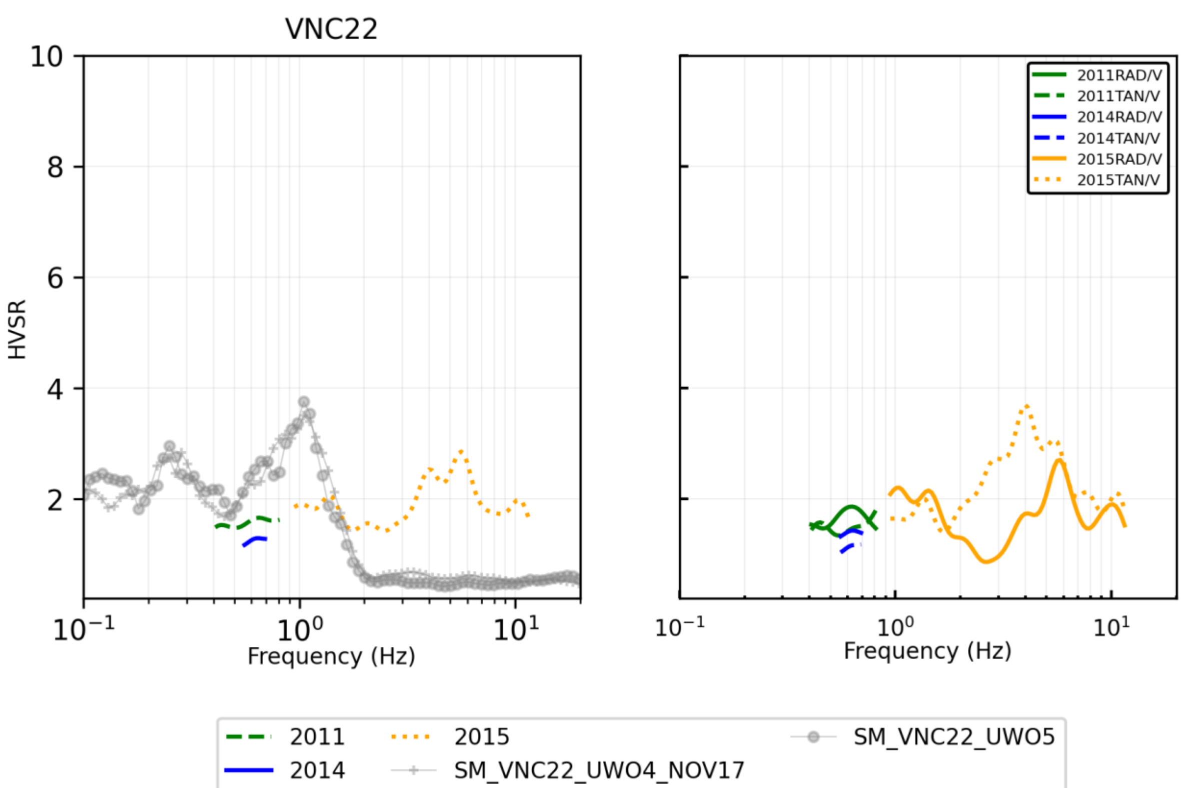
VNC22
10
8
6
4
2
HVSR
10^{-1}
10^{0}
10^{1}
Frequency (Hz)
2011RAD/V
2011TAN/V
2014RAD/V
2014TAN/V
2015RAD/V
2015TAN/V
2011
2014
2015
SM_VNC22_UWO4_NOV17
SM_VNC22_UWO5

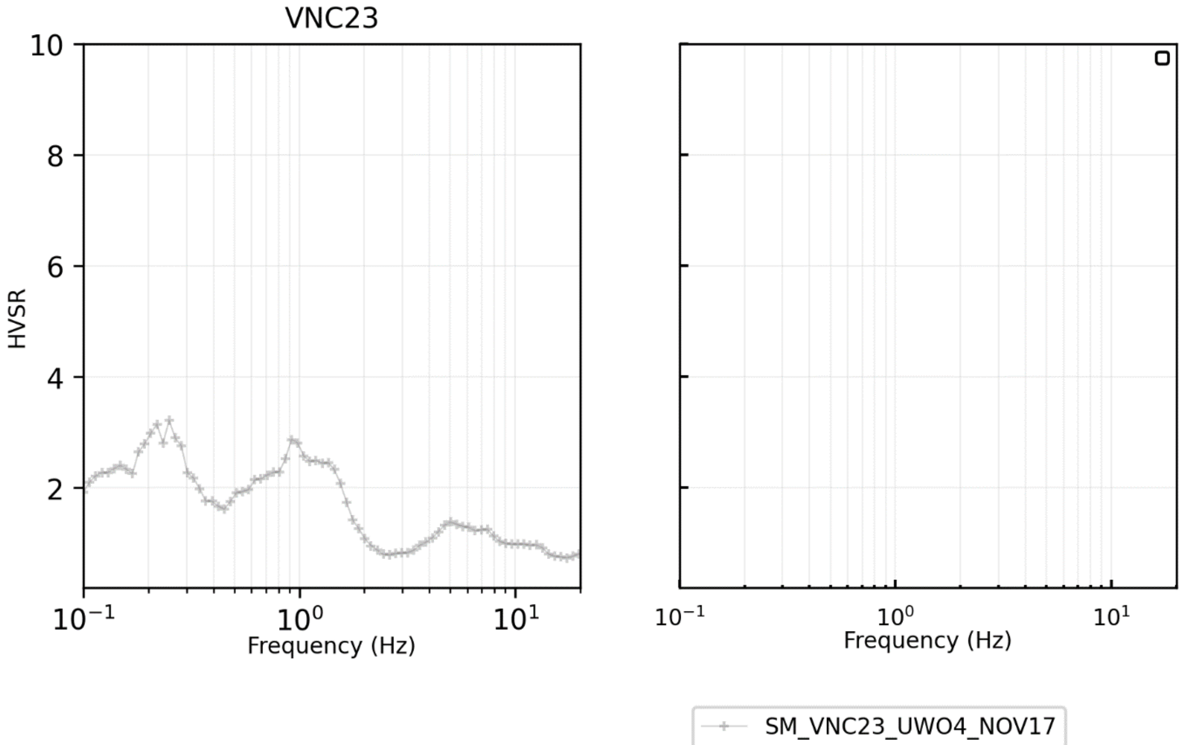
VNC23
HVSR
Frequency (Hz)
SM_VNC23_UWO4_NOV17

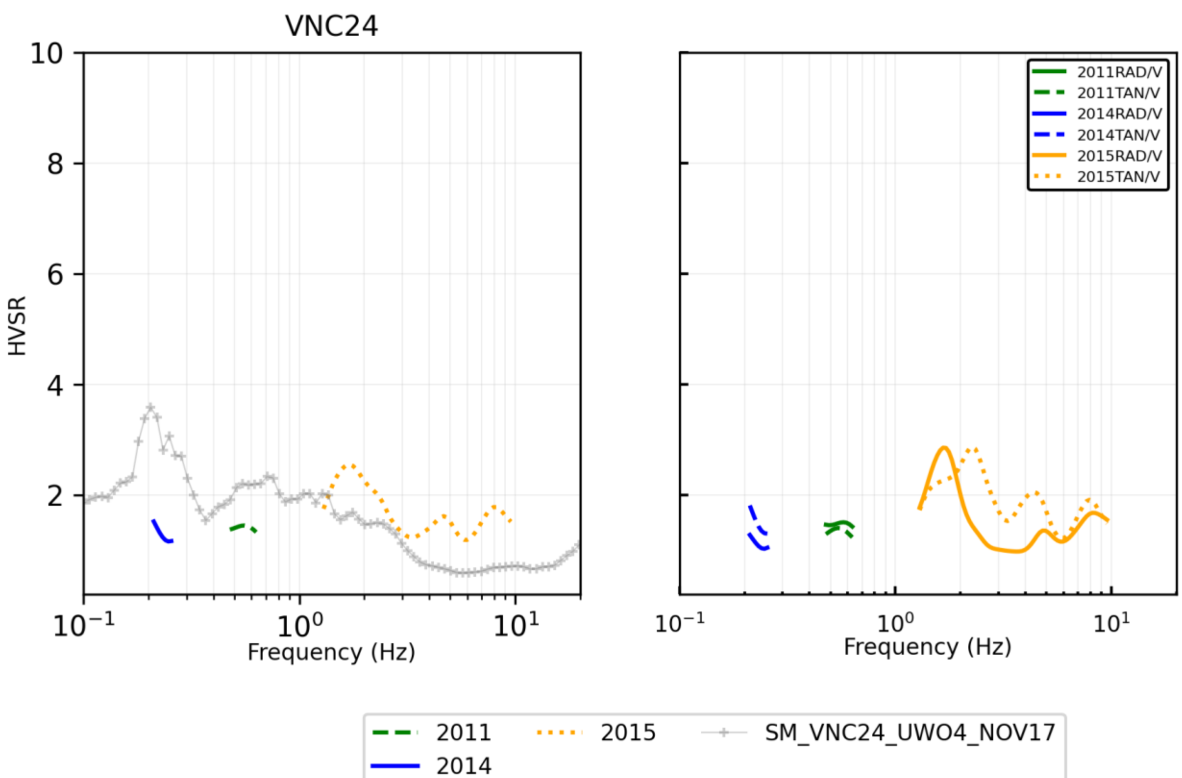
VNC24
HVSR
Frequency (Hz)
2011RAD/V
2011TAN/V
2014RAD/V
2014TAN/V
2015RAD/V
2015TAN/V
2011
2014
2015
SM_VNC24_UWO4_NOV17

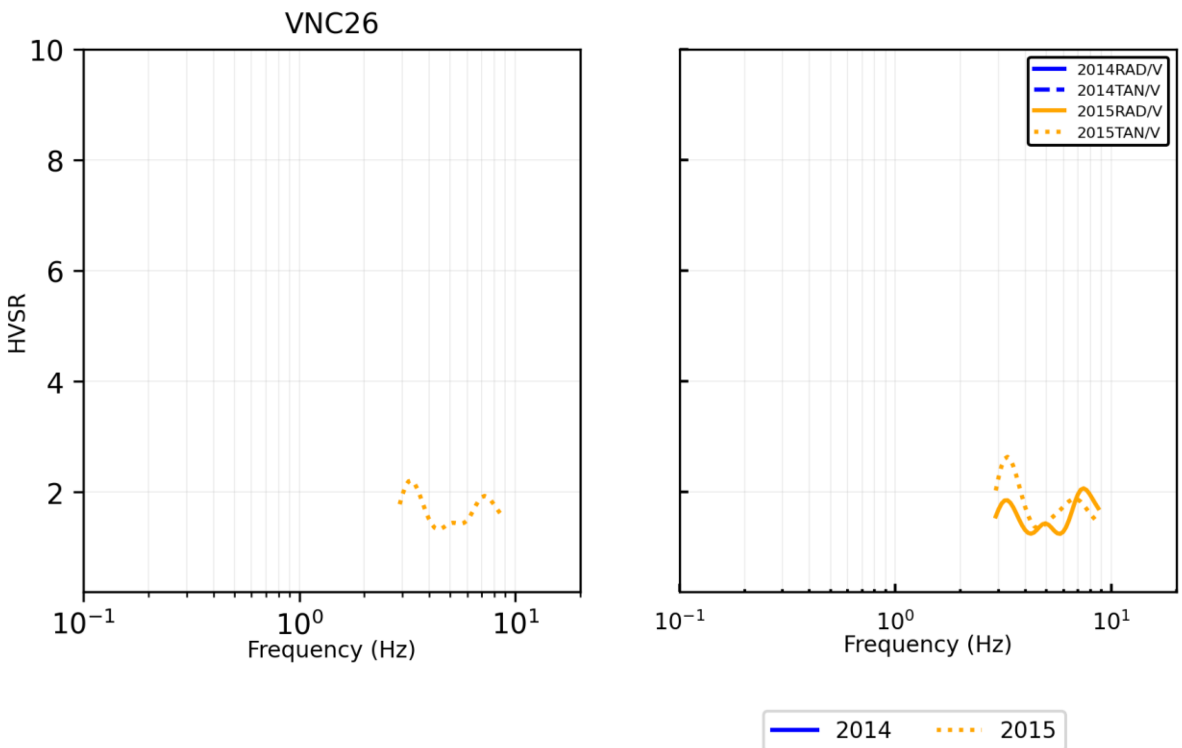
VNC26
HVSR
Frequency (Hz)
Frequency (Hz)
2014RAD/V
2014TAN/V
2015RAD/V
2015TAN/V
2014
2015

Rock Sites

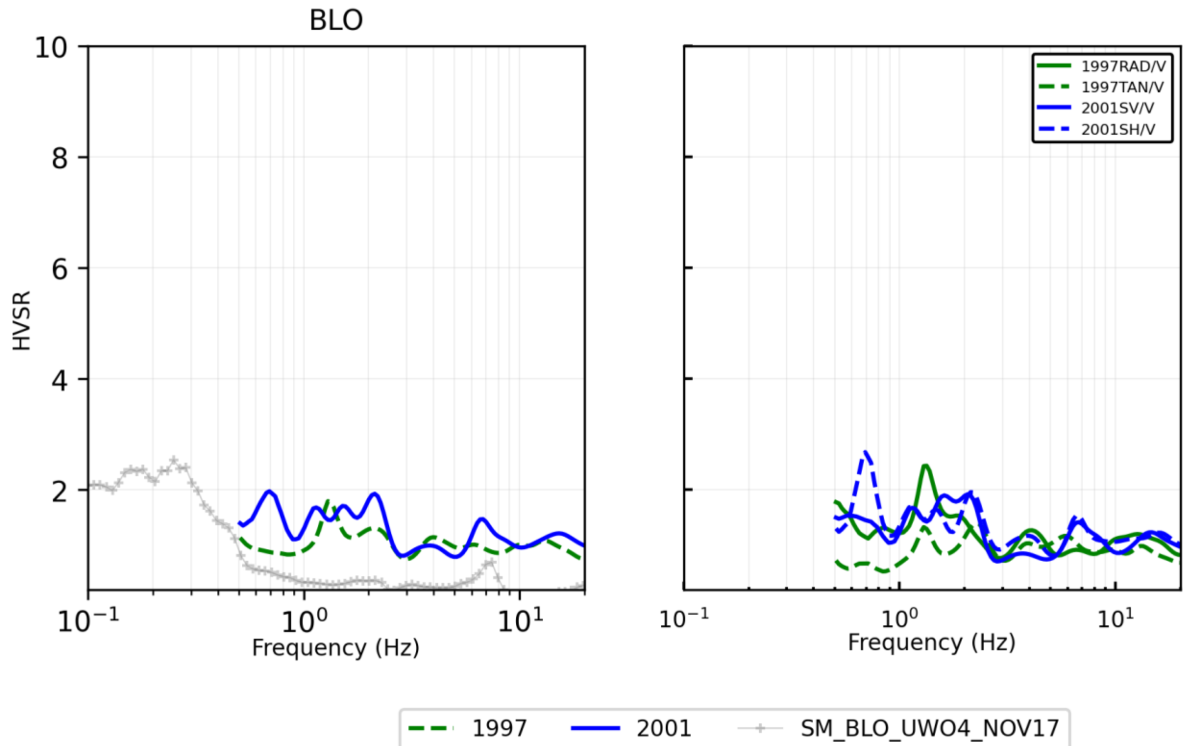
BLO
10
8
6
4
2
HVSR
10⁻¹
10⁰
10¹
Frequency (Hz)
1997RAD/V
1997TAN/V
2001SV/V
2001SH/V
1997
2001
SM_BLO_UWO4_NOV17

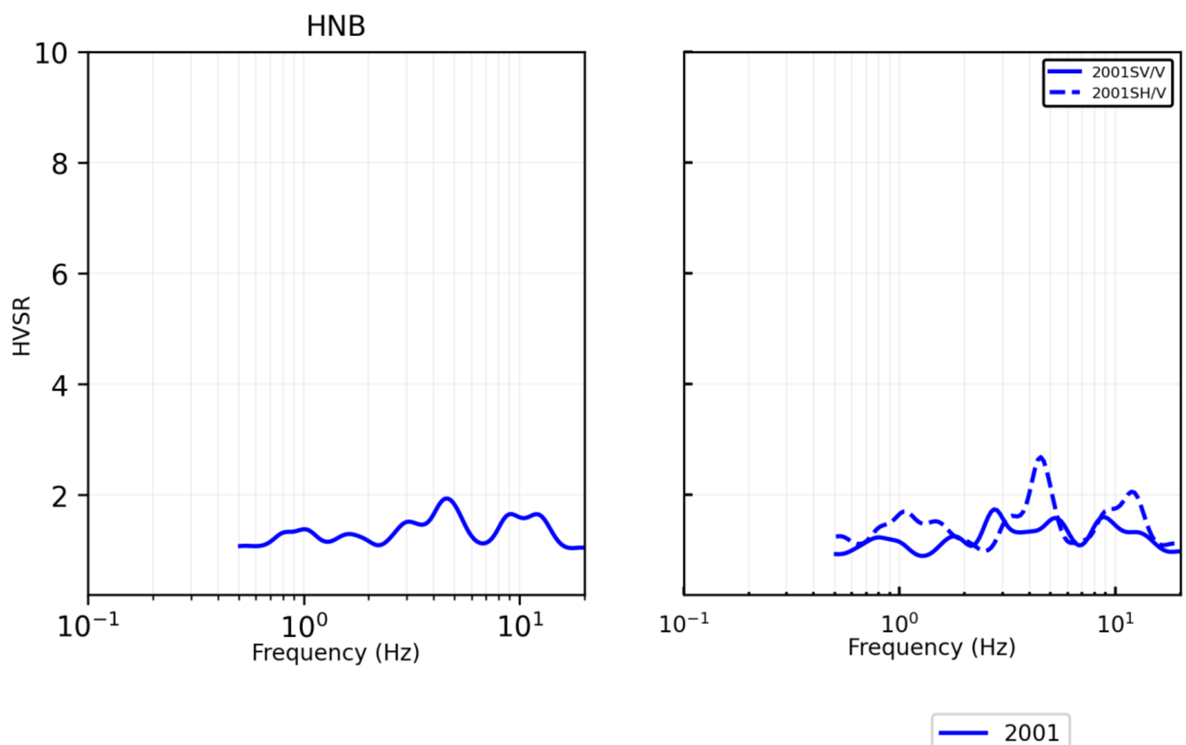
HNB
10
8
6
4
2
HVSR
10⁻¹
10⁰
10¹
Frequency (Hz)
2001SV/V
2001SH/V
2001

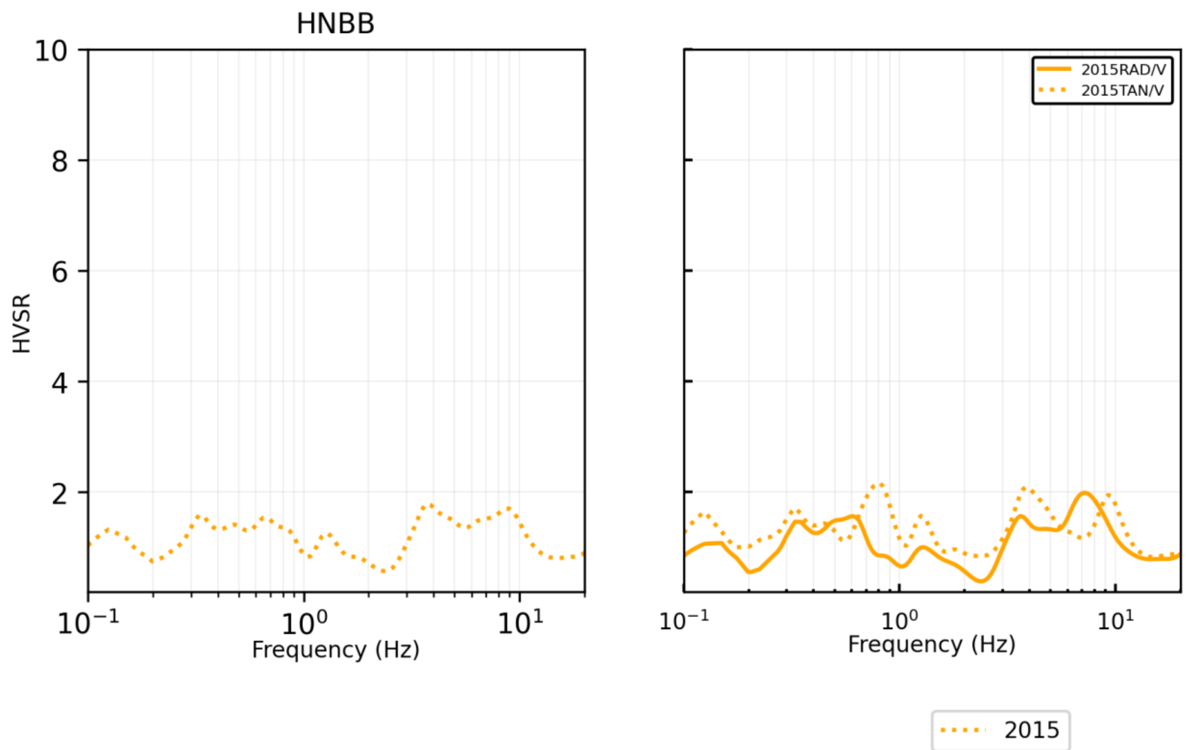

PGC is located at NRCAN (Sidney), formerly the Pacific Geoscience Centre, on Vancouver Island

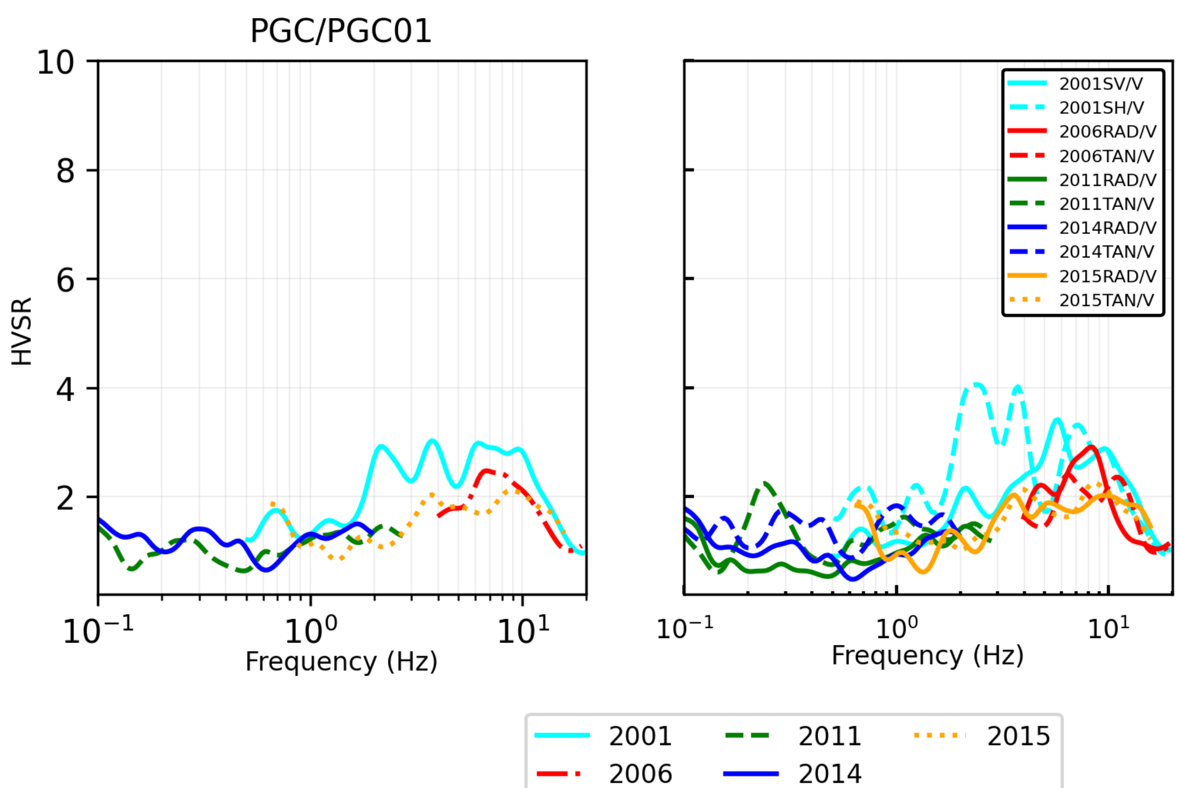

Acknowledgements

The authors would like to thank Dr. Karen Assatourians for providing the 2015 earthquake recording at HNBB station.

References

Assaf J, Molnar S, El Naggar MH, Sirohey A (2022) Seismic Site Characterization in Fraser River Delta in Metropolitan Vancouver. Soil Dynamics and Earthquake Engineering (Submitted)

Beyreuther M, Barsch R, Krischer L, et al (2010) ObsPy: A Python Toolbox for Seismology. Seismological Research Letters 81:530–533. https://doi.org/10.1785/gssrl.81.3.530

Cassidy, J.F., Rogers, G.C., and Weichert, D.H. 1997. Soil response on the Fraser Delta to the Mw=5.1 Duvall, Washington, earthquake. Bulletin of the Seismological Society of America, 87: 1354-1361

Cassidy, J.F., and Rogers, G.C. 1999. Seismic site response in the greater Vancouver, British Columbia, area: Spectral ratios from moderate earthquakes. *Canadian Geotechnical Journal*, 36(2): 195–209.

Cassidy, J.F., and Rogers, G.C. 2004. Variation in ground shaking on the Fraser River delta (Greater Vancouver , Canada) from analysis of moderate earthquakes. *13th World Conference on Earthquake Engineering*, (1010): 7.

Jackson F, Molnar S, Ghofrani H, Atkinson GM, Cassidy JF, Assatourians K (2017). Ground Motions of the December 2015 M 4.7 Vancouver Island Earthquake: Attenuation and Site Response. Bulletin of the Seismological Society of America **107**:2903–2916

Konno K, Ohmachi T (1998) Ground-motion characteristics estimated from spectral ratio between horizontal and vertical components of microtremor. Bulletin of the Seismological Society of America 88:228–241

Molnar, S., Cassidy, J.F., and Dosso, S.E. 2004. Site response studies in Victoria, BC, Analysis of Mw 6.8 Nisqually earthquake recordings and SHAKE modelling. *13th World Conference on Earthquake Engineering*, (2121).

Molnar S, Assaf J, Sirohey A, Adhikari SR (2020) Overview of local site effects and seismic microzonation mapping in Metropolitan Vancouver, British Columbia, Canada. Engineering Geology 270:. https://doi.org/10.1016/j.enggeo.2020.105568

Rogers, G.C., Cassidy, J.F., and Weichert, D.H., 1998. Variation in earthquake ground motion on the Fraser Delta from strong motion seismograph records, in Recent Geological, Geophysical, Geotechnical, and Geochemical Research, Fraser River Delta, British Columbia, (ed.) J.J. Clague, J.C. Luternauer, and D.C. Mosher; Geological Survey of Canada, Bulletin 525, 270 pp. 15.

Rosenberger, A, Beverley, K., Rogers, G., 2004. The new strong motion seismic network in southwest British Columbia, Canada, Proceedings of the 13th World Conference on Earthquake Engineering, Vancouver, Canada, 2004, Paper 2121 on CD-ROM.

Perron V, Laurendeau A, Hollender F, et al (2018) Selecting time windows of seismic phases and noise for engineering seismology applications: a versatile methodology and algorithm. Bulletin of Earthquake Engineering 16:2211–2225. https://doi.org/10.1007/s10518-017-0131-9

Weichert, D.H., and Milne, W.G. 1980. Canadian strong motion records, Canada Department of Energy, Mines and Natural Resources, Earth Physics Branch Open File Report 80-1, 89 pp